[redacted]

Technical Report No. 125

SACLANT ASW
RESEARCH CENTRE

METEOROLOGICAL DATA OF THE MILOC–BALTIC 1967 CRUISE

by

R. PESARESI

15 OCTOBER 1968

VIALE SAN BARTOLOMEO, 400
I-19026-LA SPEZIA, ITALY

[redacted]

[redacted]

TECHNICAL REPORT NO. 125

SACLANT ASW RESEARCH CENTRE
Viale San Bartolomeo 400
I 19026 - La Spezia, Italy

METEOROLOGICAL DATA OF THE MILOC-BALTIC 1967 CRUISE

By

R. Pesaresi

15 October 1968

APPROVED FOR DISTRIBUTION

Ir. M.W. van Batenburg
Director

[redacted]

Manuscript Completed:
12 August 1968

[redacted]

TABLE OF CONTENTS

List of Figures

METEOROLOGICAL DATA OF THE MILOC-BALTIC 1967 CRUISE

By

R. Pesaresi

ABSTRACT

The meteorological observations taken during a multi-ship oceanographic survey conducted in the Baltic Sea in June 1967 are reported. Derived calculations of the fluxes of momentum, sensible and latent heat, and the solar radiation are also shown.

INTRODUCTION

In June 1967 a multi-ship oceanographic survey was held in the Baltic Sea.

The SACLANTCEN Research Vessel MARIA PAOLINA G. took part in this survey. Routine oceanographic measurements were made, together with meteorological observations from the ship and from an automatic recording meteorological buoy designed and constructed at SACLANTCEN.

The geographic positions during the three phases of the cruise, together with the time schedule, are shown in Fig. 1. During phases A and C the ship was anchored in the position shown. During phase B she followed a drogue, keeping her bow to the wind.

Four sets of meteorological observations were simultaneously and continuously recorded, each set consisting of dry and wet bulb temperatures and wind speed. To emphasize the sensitivity and the precision of the measurements, the four heights at which meteorological observations were taken were as usual logarithmically spaced. These heights were chosen at 16 m and 8 m above sea level on the ship, and at 4 m and 2 m on the buoy. At the same time the solar radiation, the net radiation, the sea surface temperature, the sea temperature five metres below the surface, the relative wind direction, the ship's heading, and the radiation temperature of the sea surface were continuously recorded on board the ship.

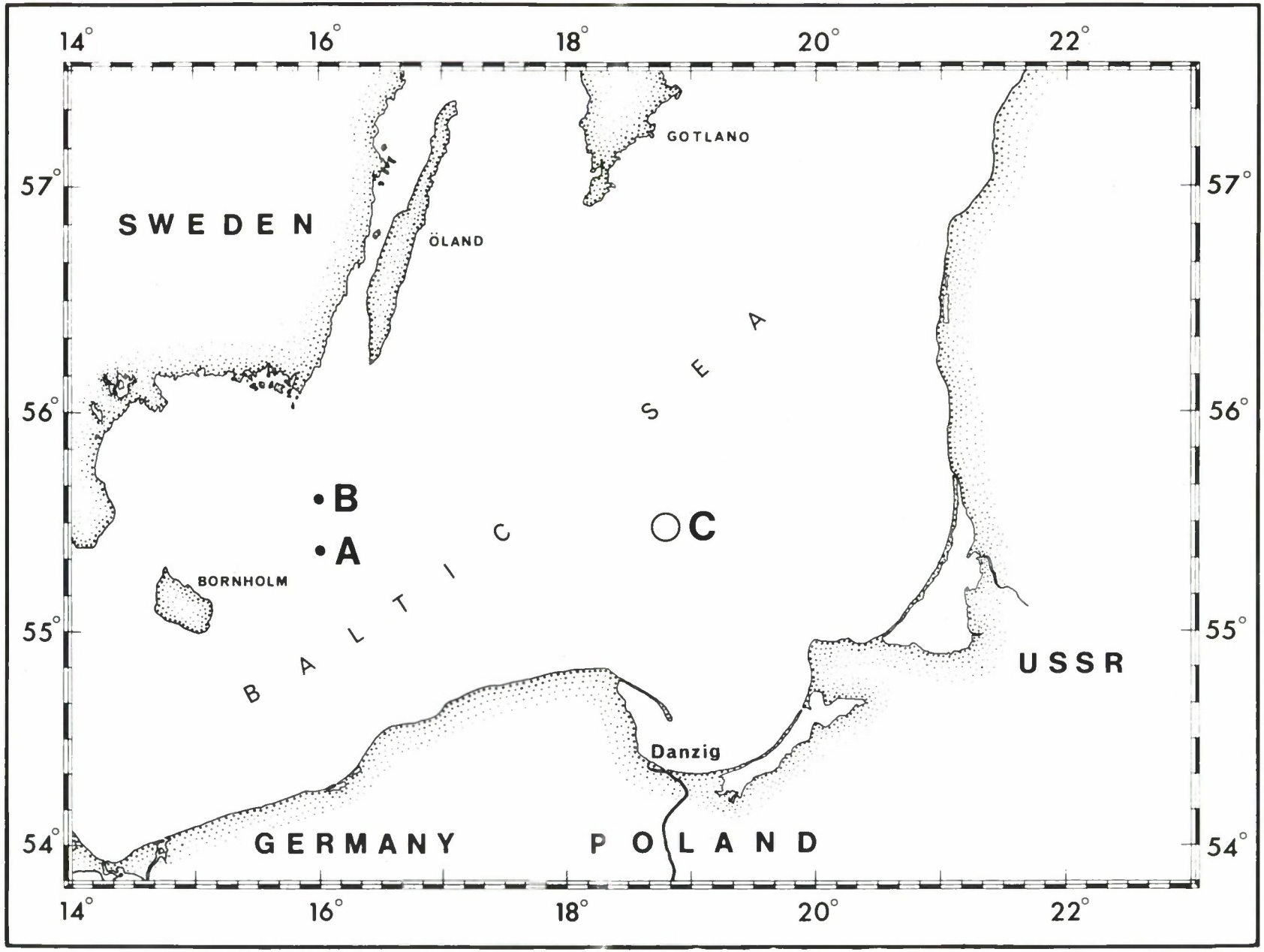

FIG. 1 LOCATION OF MEASUREMENTS: PHASE A: 6– 9 JUNE 1967
PHASE C: 13–16 JUNE 1967
PHASE B: 17–20 JUNE 1967

The primary aim of this complex set of observations was to measure the meteorological elements relevant to the calculation of the exchange of mechanical and thermal energy between the atmosphere and the sea. These fluxes, together with the solar radiation flux, directly influence the physical properties of the sea water above the thermocline, and a knowledge of their behaviour is essential to the study of that part of the ocean.

There are two main reasons why it is important to measure meteorological profiles at sea. First, because these profiles allow the evaluation of fluxes by using only the measurements made in the atmospheric boundary layer away from the interfering effects of the sea surface, the influence of which is not yet completely known. Second, they allow the study of the mechanical and thermal properties of the thin boundary layer near the sea surface that directly affect the energy transfer process through the interface. This can be done by applying the theory that relates the profiles to the fluxes, or better by measuring the fluxes by an independent method, such as the eddy correlation technique.

This report on the meteorological measurements taken during the MILOC BALTIC 1967 cruise publishes the plots, in function of time, of the elements measured, together with the results of the flux calculations and their plots.

The flux calculations are derived from the bulk properties of the atmosphere between the 16 m level and the sea surface. These calculations do not take account of the profiles that can possibly be reconstructed from the observations made at four heights, as the data measured on the buoy and on the ship do not completely agree. As explained in Chapter 3 this discrepancy may be due to instrument errors on the buoy, to the physical effect of the ship's presence on the air flow past the ship sensors, or to a combination of these causes. It would be interesting to isolate the two, in order to study the latter.

1. DISPOSITION AND ACCURACIES OF THE SENSORS

1.1 Disposition

Figure 2 shows the disposition of the sensors on the ship and the buoy. Those on the buoy consist of two sets, each comprising an aspirated thermistor psychrometer and a cup anemometer, mounted 2 metres and 4 metres above sea level. The mountings were at the ends of 1.5 m long arms extending from the buoy's mast. The buoy was stabilized by a 400 kg weight rigidly attached 8 m below it.

The ship carried two similar sets of instruments: one set at 8 m above sea level being mounted at the end of an aluminium lattice boom extending 17 m forward from the bow, and the other set at 16 m above sea level being mounted on a boom 5 m forward of the crow's nest on the foremast. The 8-m high installation also included a radiation balance probe. A standard ship anemometer of the propeller type, mounted on the foremast, sensed the relative wind direction as well as the wind speed. A gimbal-mounted Kipp solarimeter and a Barnes radiation thermometer were mounted on top of the foremast. A small float towed from the ship's bow boom supported two thermometers, one at the sea surface and the other 5 m below.

1.2 Instrument Accuracy

The ship thermometers were calibrated before and after the cruise; Fig. 3 shows the difference between these calibrations, over

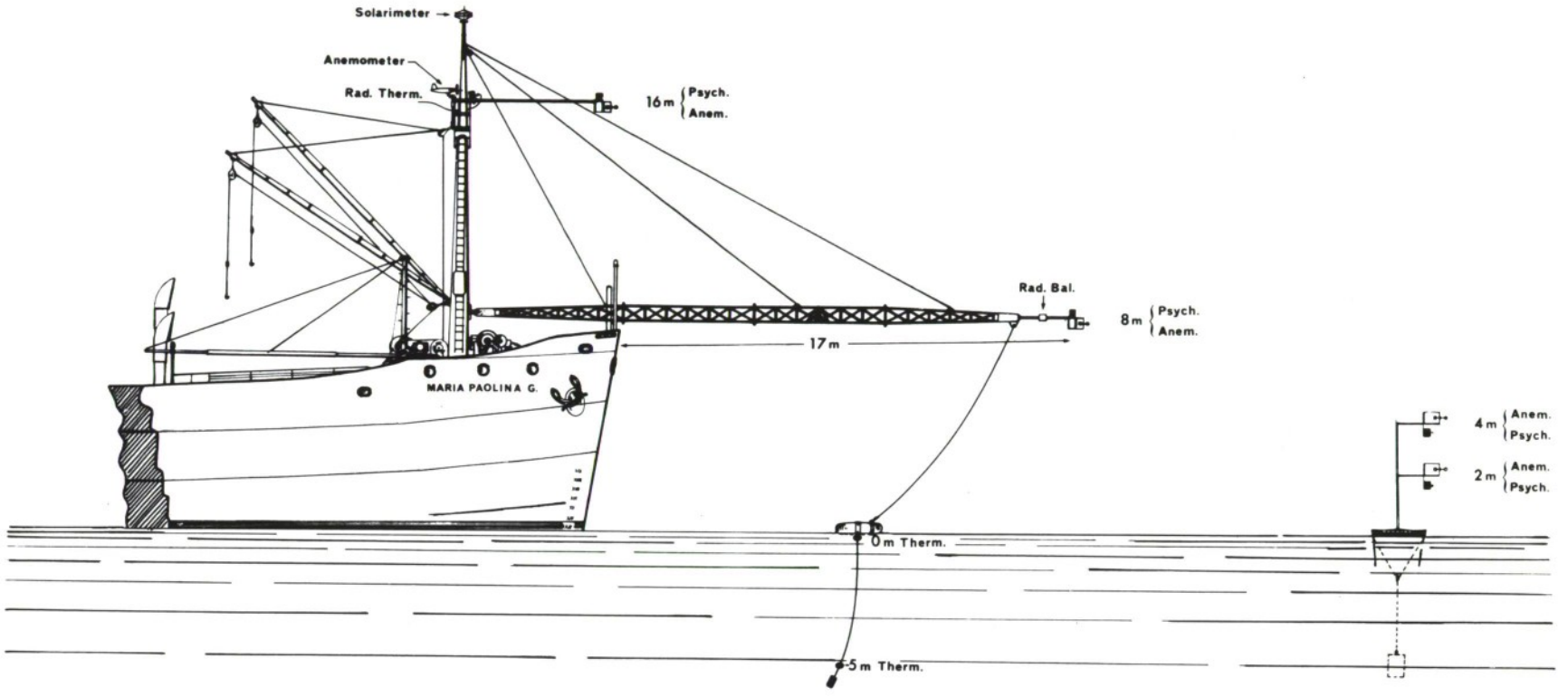

FIG. 2 LOCATION OF SENSORS ON THE SHIP AND ON THE BUOY

the range of temperatures encountered during the cruise. For data reduction purposes the first calibration was used. During the measurements reported the standard deviation of the readings (referred to as twenty-minute average values) of a reference channel on the recording system was calculated to be 0.001°C. The accuracy of the recording system itself was estimated to be within 0.019°C, both in the absolute and in the relative measurements, not including the calibration shift.

As the buoy was lost at the end of the cruise, its thermometers were only calibrated before the cruise. However, from past experience they are estimated to be less stable than the differences shown in Fig. 3, but generally by no more than a factor of two; obviously individual sensors may shift much more. During the tests on the recording and reading system of the buoy, the standard deviation was calculated to be 0.007°C. The accuracy of the temperature values reported cannot be firmly assessed as the electronics and some standards within the buoy could not be tested and checked after the cruise. However, the accuracy can be estimated to be within 0.02°C for the relative measurements, not including any calibration shift.

The anemometers were calibrated only before the cruise, as those used on board the ship were damaged during removal, and those on the buoy were lost. Their stability and accuracy are estimated to be within 1%. The reading precision is, in both cases, plus or minus one revolution of the anemometer shaft in twenty minutes, that is 0.0014 m/s.

The radiation thermometer shows a difference between the two calibrations of about 1°C, reflecting the poor quality of the instrument. In view of this calibration shift its measurements

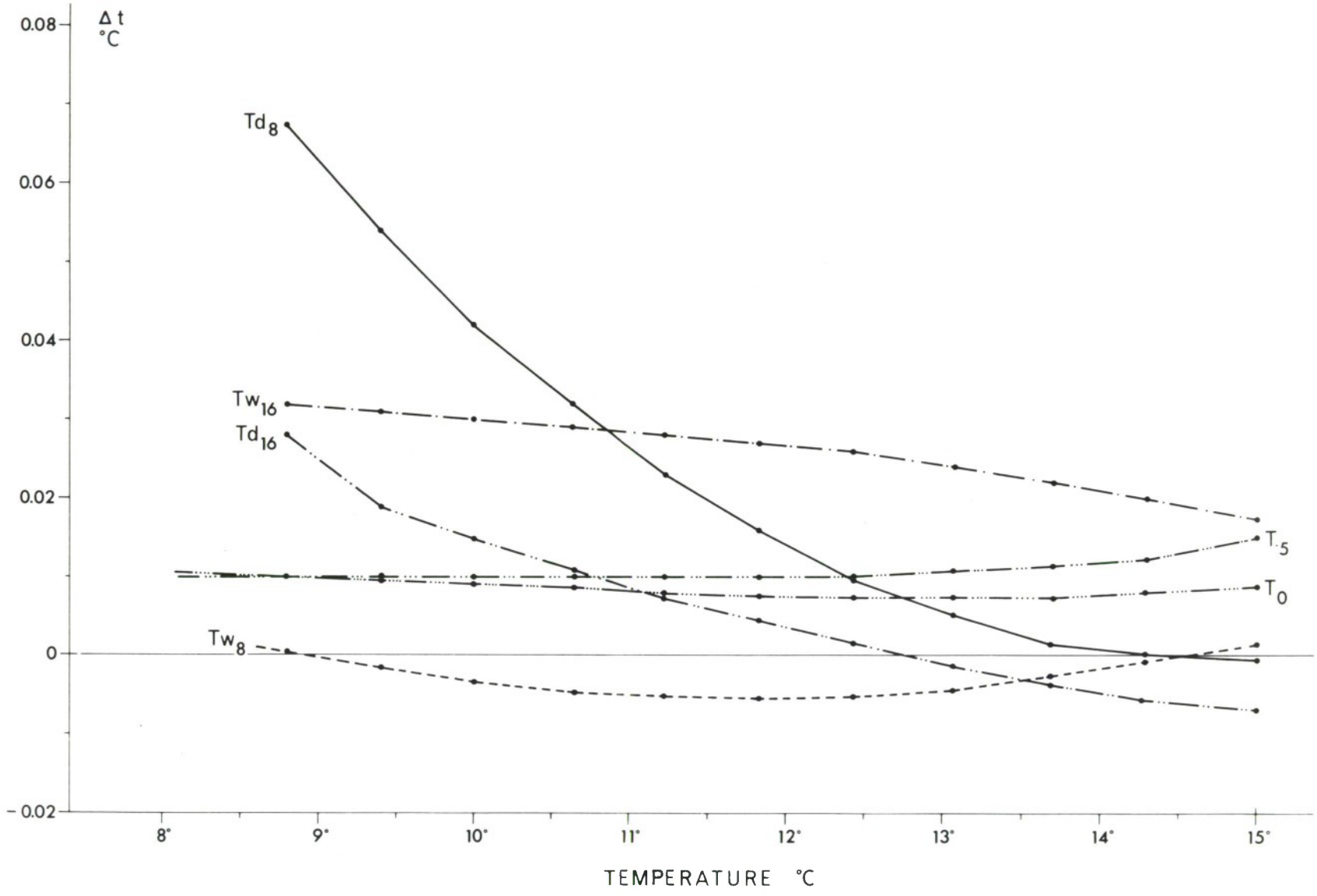

FIG. 3 SHIFT IN THE CALIBRATION OF THE SHIP THERMOMETERS

can be used only for short-term comparisons. During the data reduction, the first calibration was used.

The solarimeter was calibrated with a standard Ångström pyrheliometer before the cruise. The accuracy of its readings is essentially determined by the contact potentials arising in the junctions between the instrument and the recorder, and was estimated to be within 0.01 cal/(cm^2 . min), that is 0.6 cal/cm^2 in the one-hour values of the fluxes.

The same considerations apply to the net radiation sensor, but it must be remembered that the instrument was not always horizontal and, moreover, its field of view was partly obstructed by the ship.

2. DATA REDUCTION AND PRESENTATION (See Appendix A)

Data from both the ship and the buoy were recorded once a minute. They were first edited for large deviations and then filtered by a low-pass numerical filter, the frequency response characteristics of which are shown in Fig. 4.

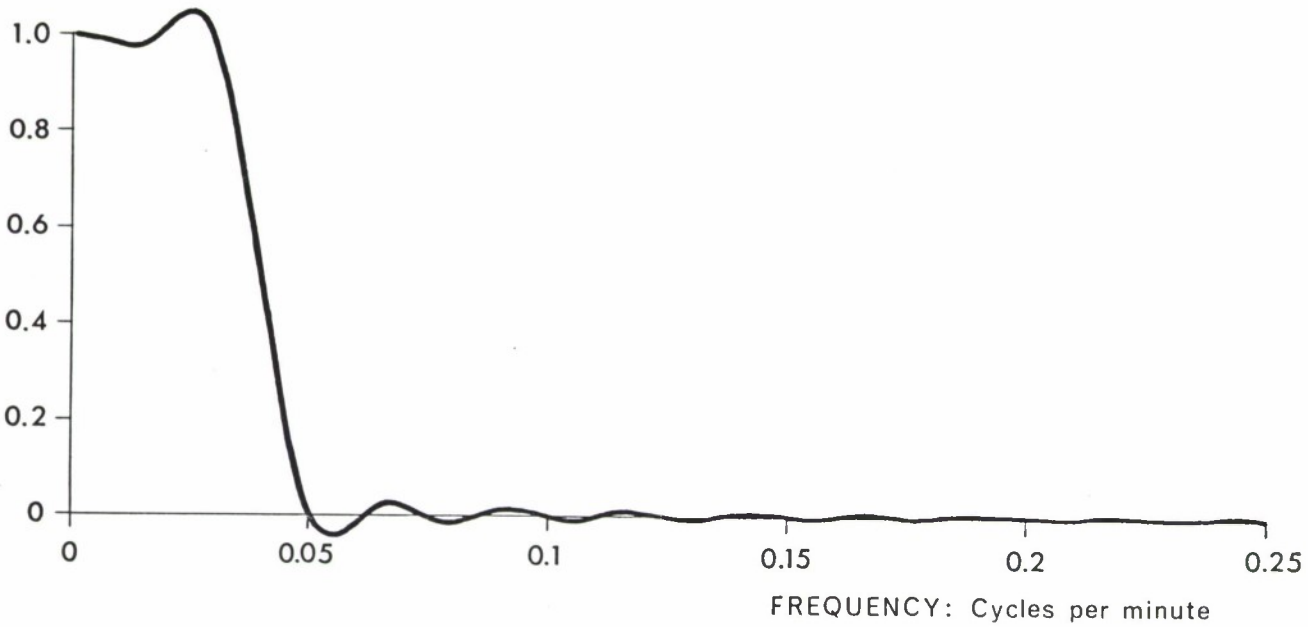

FIG. 4 FREQUENCY RESPONSE OF THE LOW-PASS NUMERICAL FILTER

After filtering, every tenth value was extracted and plotted to give the graphical presentation shown in App. A. (The values themselves are available on punched paper tape for those who are interested.) Examples of the printout are given in App. A.

The temperatures plotted are approximate potential temperatures, which have been obtained by adding the dry adiabatic lapse rate of 0.0098°C/m to the actual temperature measured.

3. METEOROLOGICAL PROFILES

Figure 5 shows a typical example (8 June 1967, 0120. See printout in App. A) of actual values of potential temperature and wind speed, measured at 2 m and 4 m on the buoy and at 8 m and 16 m on the ship. The solid lines represent the profiles of potential temperature and wind speed calculated according to the aerodynamic theory of the turbulent transfer of energy in the atmospheric boundary layer ("profile theory"). The dashed lines show, for comparison, the potential temperature and wind speed profiles calculated according to the bulk aerodynamic theory (with constant roughness parameter), using the 16 m and sea-surface observations ("bulk theory").

It can be clearly seen that the profiles obtained from the measurements from the ship and from the buoy do not completely coincide. Even though the difference is not large, it is larger than the measurement tolerance and appears consistently over all the profiles. There may be two explanations for this systematic difference. It could be caused by the instruments, due to a shift in the calibration of all the buoy probes, or to the electronics and the automatic recording system of the buoy itself. (As the buoy was lost it was not possible to check the calibration of the sensors and the electronics after the cruise.) The second possible explanation is that the ship disturbs and distorts the air flow passing above it. Therefore, the ship sensors would be measuring in air that had been carried to a height above its normal level.

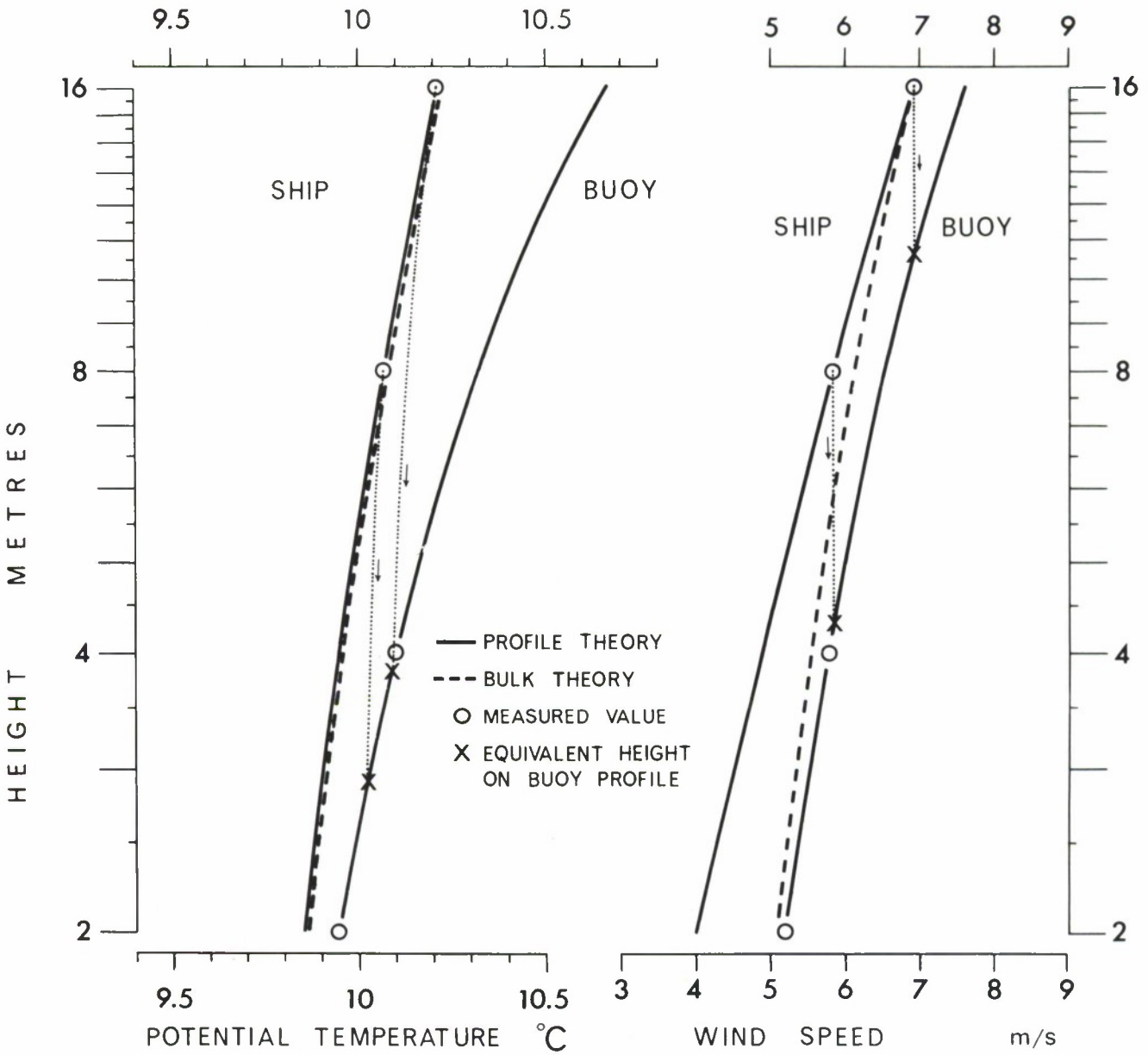

FIG. 5 PROFILES OF POTENTIAL TEMPERATURE AND WIND SPEED MEASURED AT 2 m AND 4 m ON THE BUOY AND AT 8 m AND 16 m ON THE SHIP. (8 JUNE 1967 0120)

The lack of coincidence between ship and buoy measurements is further illustrated in Figs. 6 and 7. These figures show, for a 24 hour period (8 June), the heights at which the values recorded on the ship, at 16 m and 8 m respectively, occur on the profiles calculated from the buoy measurements. (An example of these equivalent heights is given on Fig. 5.) The solid lines indicate the equivalent heights of the wind speed values, the dashed lines those of the potential temperature. Gaps are either because of missing data or because the equivalent height is less than 2 m.

The wind speed curves on both Figs. 6 and 7 indicate that the speeds recorded on the ship consistently occur at much lower heights on the buoy data profile. This suggests that the differences may be due entirely to the disturbance of the ship.

The temperature curves on both Figs. 6 and 7 also show that the temperatures recorded on the ship consistently occur at lower heights on the buoy data profile. This could again be explained by ship disturbance, but as the equivalent heights for the temperatures are much lower than the corresponding equivalent heights for the wind speeds — especially in Fig. 6 — these differences could be due to instrumental shifts and also, to a minor extent, to an inadequacy of the profile theory in stable air. It might be possible to isolate these effects by a careful analysis of the values involved.

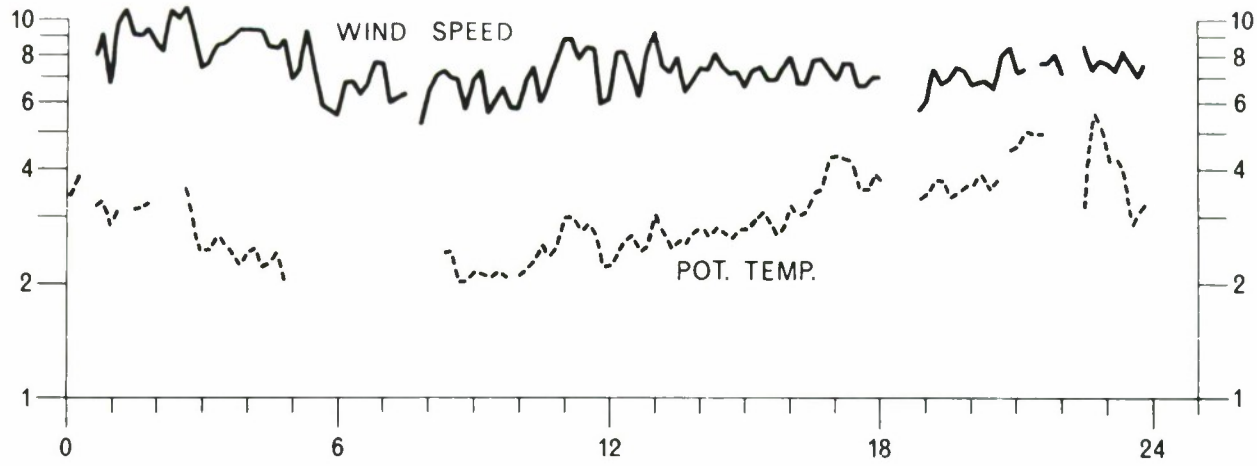

FIG. 6 HEIGHTS AT WHICH THE WIND SPEED AND THE TEMPERATURE SENSED AT 16 m ON THE SHIP, CORRESPOND TO THE PROFILES PASSING THROUGH THE BUOY MEASUREMENT

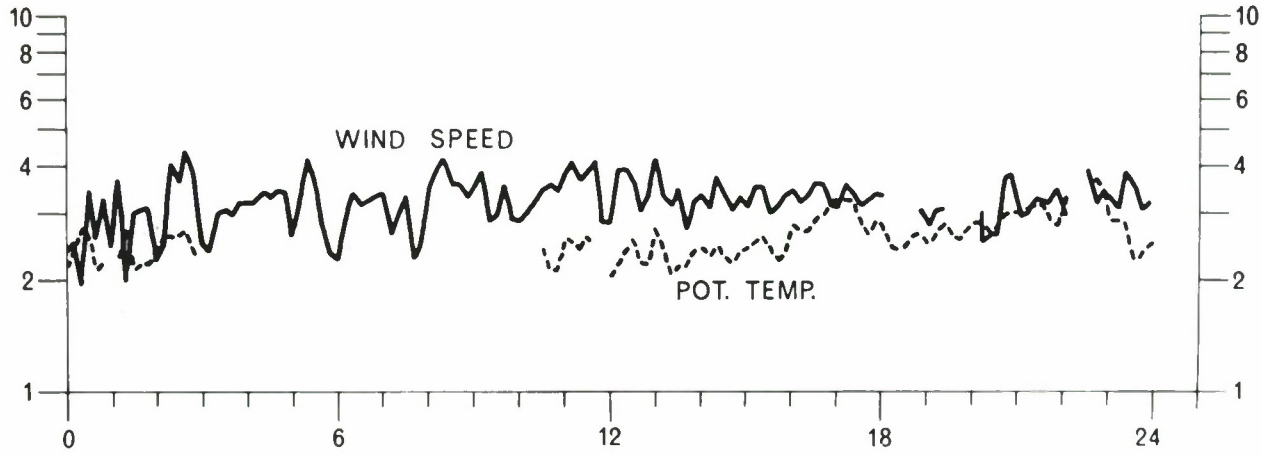

FIG. 7 HEIGHTS AT WHICH THE WIND SPEED AND THE TEMPERATURE SENSED AT 8 m ON THE SHIP, CORRESPOND TO THE PROFILES PASSING THROUGH THE BUOY MEASUREMENT

4. FLUX CALCULATIONS (See Appendix B)

Since the measurements taken from the ship and those taken from the buoy do not completely agree, as was explained in Ch. 3, the meteorological profiles cannot be reconstructed reliably. Therefore, the flux calculations reported here are not derived by the profile method but by the bulk method, that is by using the meteorological observations at 16 m on the ship and the sea surface temperature.

The use of the bulk method implies a knowledge of the thermal and mechanical properties of the boundary layers adjacent to the sea surface, or, in a more simplified formulation, of the roughness parameter (z_0) of the sea surface itself.

As some of the problems of the influence of the meteorological and oceanographic parameters on the physical properties of the sea surface still remain unsolved, the fluxes were calculated by taking a constant roughness parameter, the value of which was derived from the work of Brocks in the Baltic Sea [Ref. 1].

The only correction made to the standard bulk method was to take into account the stability of the air. This was done according to a working model based on the most recent published experimental work on the influence of atmospheric stability

on the transfer coefficients. Similar models are described by Deardorff [Ref. 2] and Paulson [Ref. 3].

The three formulae used for calculating the momentum flux (or shear stress) τ, the sensible heat flux H, and the latent heat flux due to evaporation E, according to the bulk aerodynamic theory with constant roughness parameter (z_o), are respectively as follows:

$$\tau = \rho\gamma K_m u^2_z$$

$$H = \rho c_p \gamma K_h (\theta_z - \theta_o) u_z$$

$$E = \rho L_v \left(\frac{\partial q}{\partial e}\right)_p K_h (e_z - e_o) u_z$$

where

ρ : density of the air = 1.26×10^{-3} g/cm^3

γ : drag coefficient = 1.65×10^{-3}

The drag coefficient is expressed as:

$$\gamma = \left[k/\left(\log_e z/z_o\right)\right]^2$$

where

k : Von Karman constant = 0.41

z : height of the observations = 8×10^2 cm

z_o : roughness parameter = 3.3×10^{-2} cm

c_p : specific heat of the air at constant pressure = 0.24 cal/(g · °C)

L_v : latent heat of vaporization of water = 591.7 cal/g

$\left(\frac{\partial q}{\partial e}\right)_p$: rate of change of specific humidity with vapour pressure at constant pressure = 6.12×10^{-4} (g/g)/mb

u : wind speed in m/s

θ : potential temperature in °C

e : water vapour pressure in mb

Suffixes z and o refer respectively to the heights of observation z and the sea surface.

K_m and K_h are correction coefficients, dependent on stability parameters and calculated according to the bulk aerodynamic theory.

The constants were calculated at 10°C mean air temperature, 1025 mb mean air pressure.

Using the above-listed values for the constants, the bulk formulae become:

Momentum Flux: $\tau = 2.074 \times 10^{-2} K_m u_z^2$ dyn/cm²

Sensible Heat Flux: $H = 2.987 \times 10^{-3} K_h(\theta_z - \theta_o) u_z$ cal/(cm²·min)

Latent Heat Flux: $E = 4.507 \times 10^{-3} K_h(e_z - e_o) u_z$ cal/(cm²·min)

The Solar Radiation Flux (S) was measured directly. The fluxes are taken to be positive when the flow of energy is towards the sea surface.

Fluxes were calculated from the filtered values recorded on the ship every tenth minute. The six values per hour were totalled to give the hourly flux per square centimetre, which are then expressed in g/(cm·s) for the flux of momentum and in cal/cm^2 for the other fluxes. These hourly fluxes are presented in tables and graphs in App. B.

The accuracy of these calculations depends entirely on the accuracy of the value of roughness length that is used. More precisely it depends on how validly the empirical theory from which the roughness length is derived represents the physical processes involved in the transfer of energy at the air-sea interface. This subject is still highly controversial [Refs. 4, 5, 6, 7 and 8] and reported values of the roughness length vary by several orders of magnitude. For these reasons the calculated fluxes may be inaccurate by more than a factor of two.

This inaccuracy, implicit in the "bulk" aerodynamic method, with its constant roughness length, supports the efforts spent in endeavouring to measure the meteorological profiles, which can give much more accurate values of the fluxes.

REFERENCES

1. K. Brocks, Probleme der Maritimen Greuzschicht der Atmosphäre Deutscher Wetterdienst Berichte, Vol. 12 No. 91, 1963, pp.34-46.

2. J.W. Deardorff,Dependence of Air-sea Transfer Coefficients on Bulk Stability. J. Geophysical Res., Vol. 73, 1968, pp.2549-57.

3. C.A. Paulson, Profiles of Wind Speed, Temperature and Humidity over the Sea. Sci. Rept. N.S.F., G.P. 2418, Dept. of Atm. Sci. Univ. of Washington, 1967.

4. S.A. Kitaigorodsky and YU. A. Volkov, On the Roughness Parameter of the Sea Surface, and the Calculation of Momentum Flux in the Near Water Layer of the Atmosphere. Izv. Acad. Sci. USSR, Atmospheric and Oceanic Physics. (English Transl.) Vol. 1, 1965, pp.566-574.

5. S.A. Kitaigorodsky and YU. A. Volkov, Calculation of Turbulent Heat and Humidity Fluxes in an Atmospheric Layer Near a Water Surface. Izv. Acad. Sci. USSR, Atmospheric and Oceanic Physics. (English Transl.) Vol. 1, 1965, pp.774-783.

6. E.B. Kraus, Aerodynamic Roughness Over the Sea Surface. J. Atmospheric Sci., Vol. 23, 1966, pp.443-445.

7. E.B. Kraus, Wind Stress Along the Sea Surface. Advances in Geophysics, Vol. 12, pp.213-255, Academic Press Inc. 1967.

8. H.U. Roll, Physics of the Marine Atmosphere. Academic Press Inc., 1965.

APPENDIX A

PROCESSED DATA

The plots of processed data for 6-9, 13-20 June record the following:

Solar Radiation (sol.)

Water Vapour Pressure (e) at 16 m, 8 m, 4 m, and 2 m

Potential Temperature (t) at 16 m, 8 m, 4 m, 2 m, 0 m, and -5 m

Radiation Temperature (rdt) at 0 m

Wind Speed (w) at 16 m, 8 m, 4 m, and 2 m
(the plot w'_{16} is that of the propellor anenometer)

The plots of each set of data have been staggered to avoid overlaps. The scale shown for each set refers to the lowest plot; reference positions for the other plots are indicated alongside.

An example of the computer printout of the processed data (0000 to 0550 on 8 June 1967) is given after the plots.

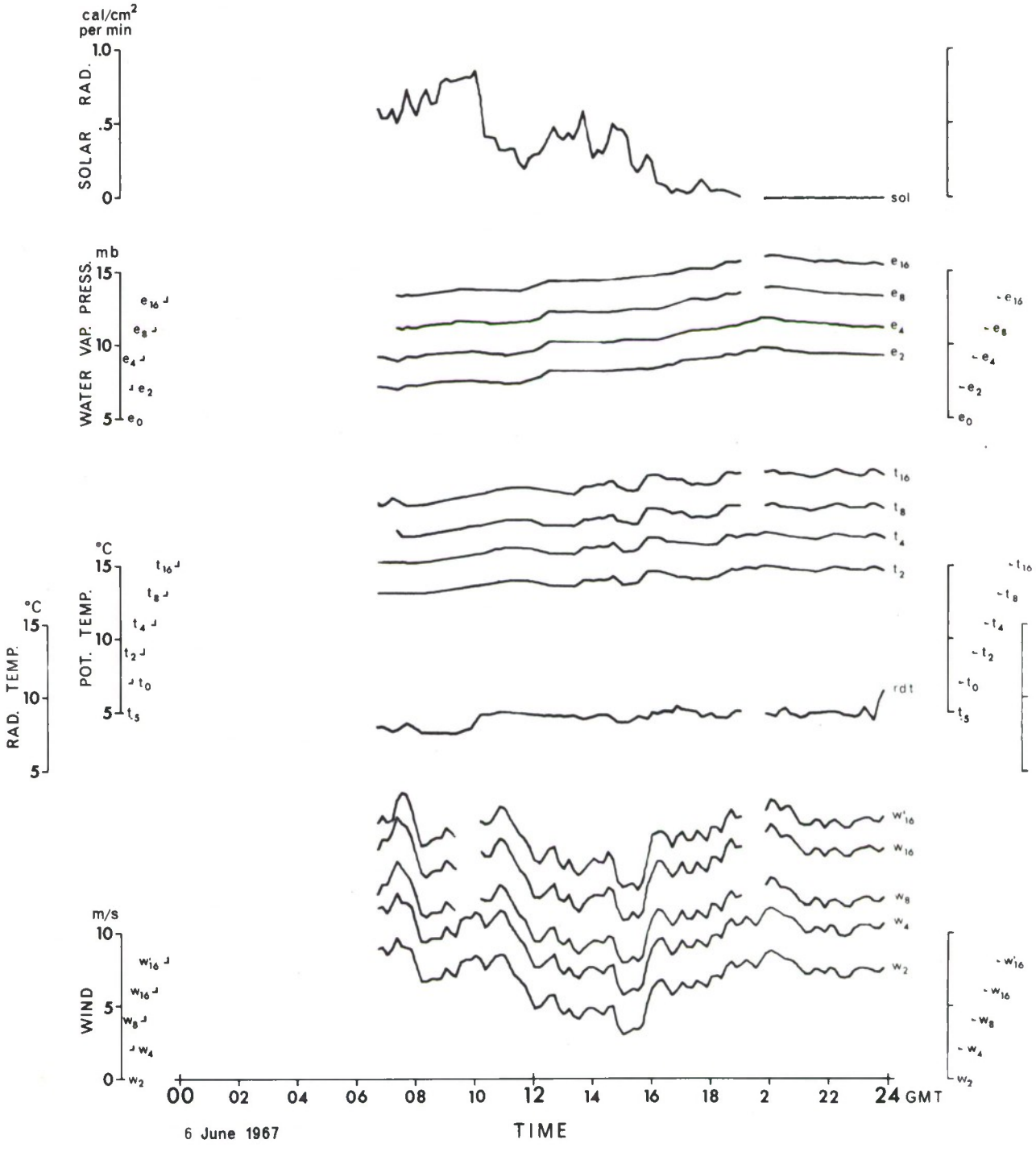
cal/cm² per min
SOLAR RAD.
1.0
.5
0
sol
mb
WATER VAP. PRESS.
15
10
5
e16
e8
e4
e2
e0
°C
POT. TEMP.
t16
t8
t4
t2
t0
t5
rdt
RAD. TEMP.
m/s
WIND
w'16
w16
w8
w4
w2
00
02
04
06
08
10
12
14
16
18
2
22
24 GMT
6 June 1967
TIME

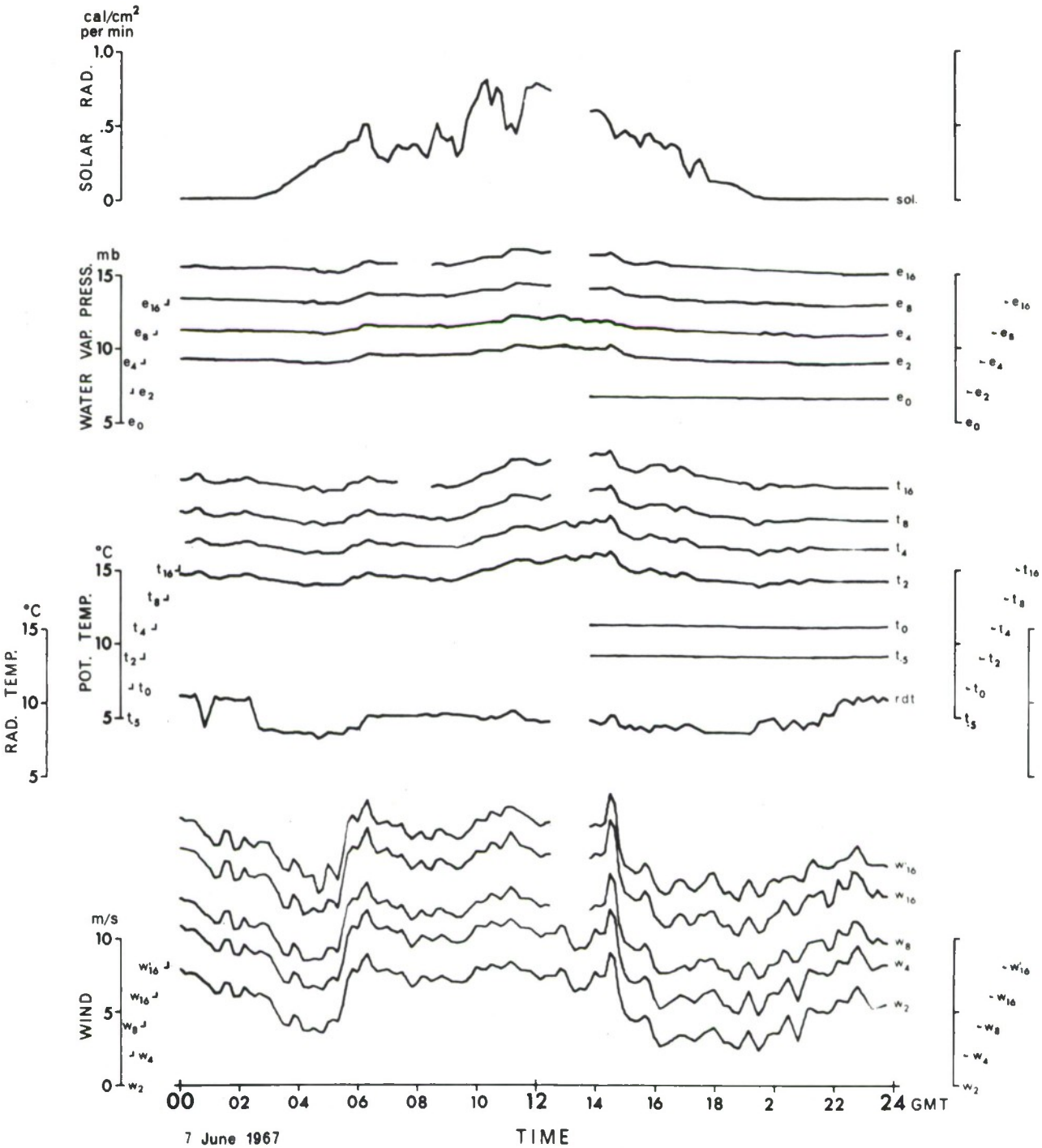
cal/cm² per min
SOLAR RAD.
1.0
.5
0
sol.
mb
WATER VAP. PRESS.
15
10
5
e16
e8
e4
e2
e0
°C
POT. TEMP.
t16
t8
t4
t2
t0
t5
rdt
RAD. TEMP.
m/s
WIND
w16
w8
w4
w2
00
02
04
06
08
10
12
14
16
18
2
22
24 GMT
7 June 1967
TIME

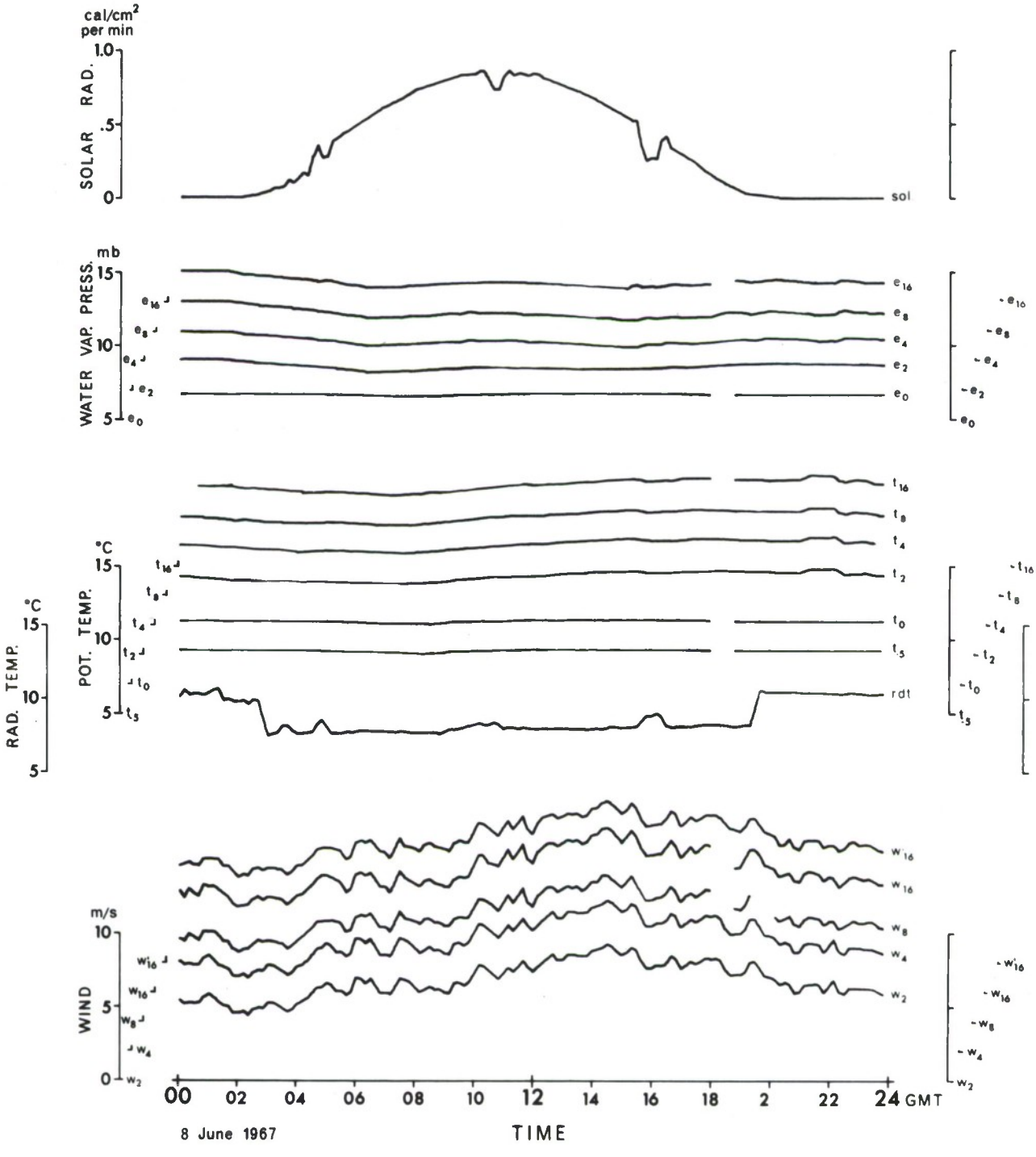
cal/cm² per min
SOLAR RAD.
1.0
.5
0
sol
mb
WATER VAP. PRESS.
15
10
5
e16
e8
e4
e2
e0
°C
POT. TEMP.
t16
t8
t4
t2
t0
t5
rdt
RAD. TEMP.
m/s
WIND
w16
w8
w4
w2
00
02
04
06
08
10
12
14
16
18
2
22
24 GMT
8 June 1967
TIME

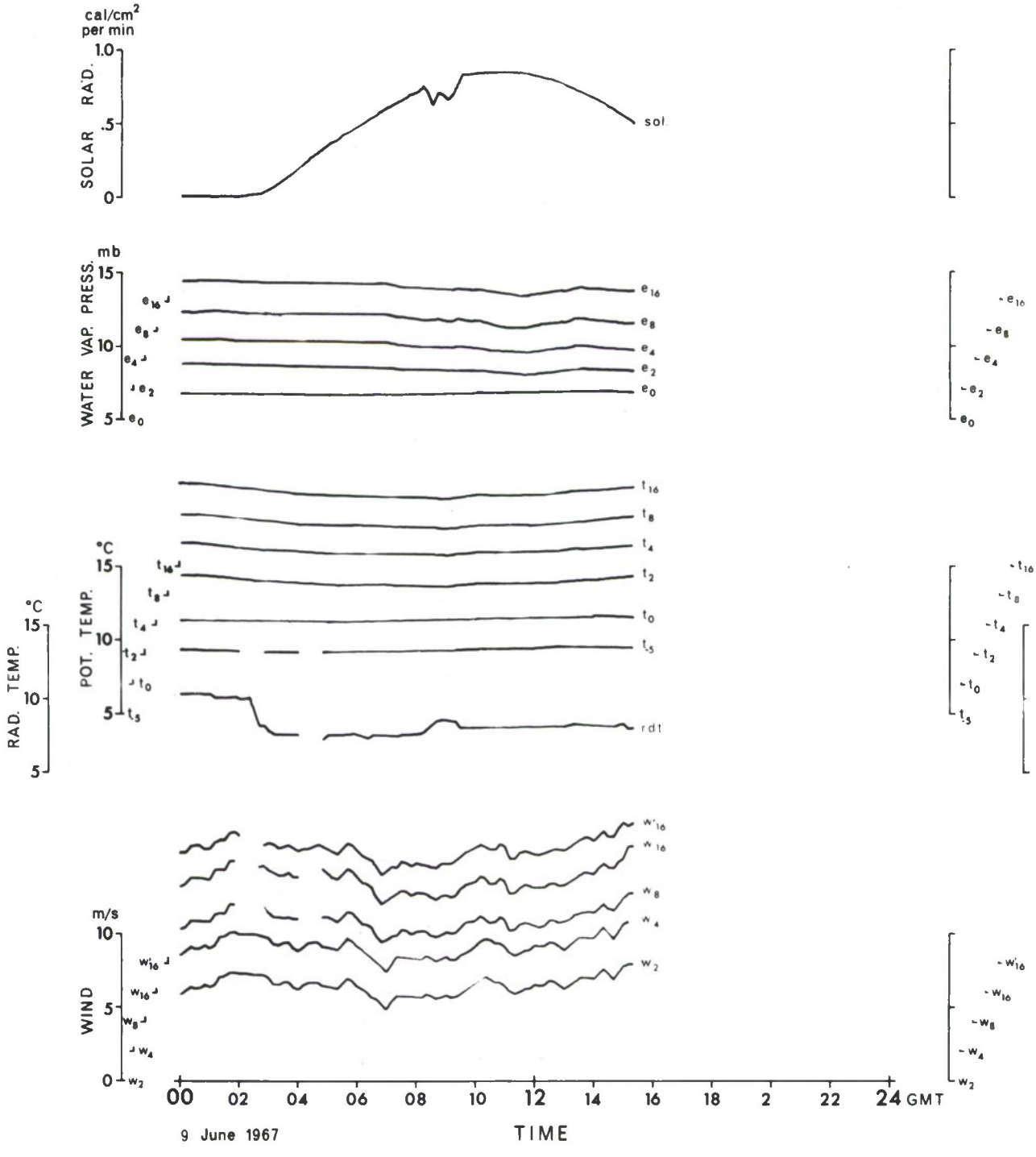
cal/cm² per min
SOLAR RAD.
1.0
.5
0
sol
mb
WATER VAP. PRESS.
15
10
5
e16
e8
e4
e2
e0
°C
POT. TEMP.
t16
t8
t4
t2
t0
t5
rdt
RAD. TEMP.
m/s
WIND
w'16
w16
w8
w4
w2
00
02
04
06
08
10
12
14
16
18
2
22
24 GMT
9 June 1967
TIME

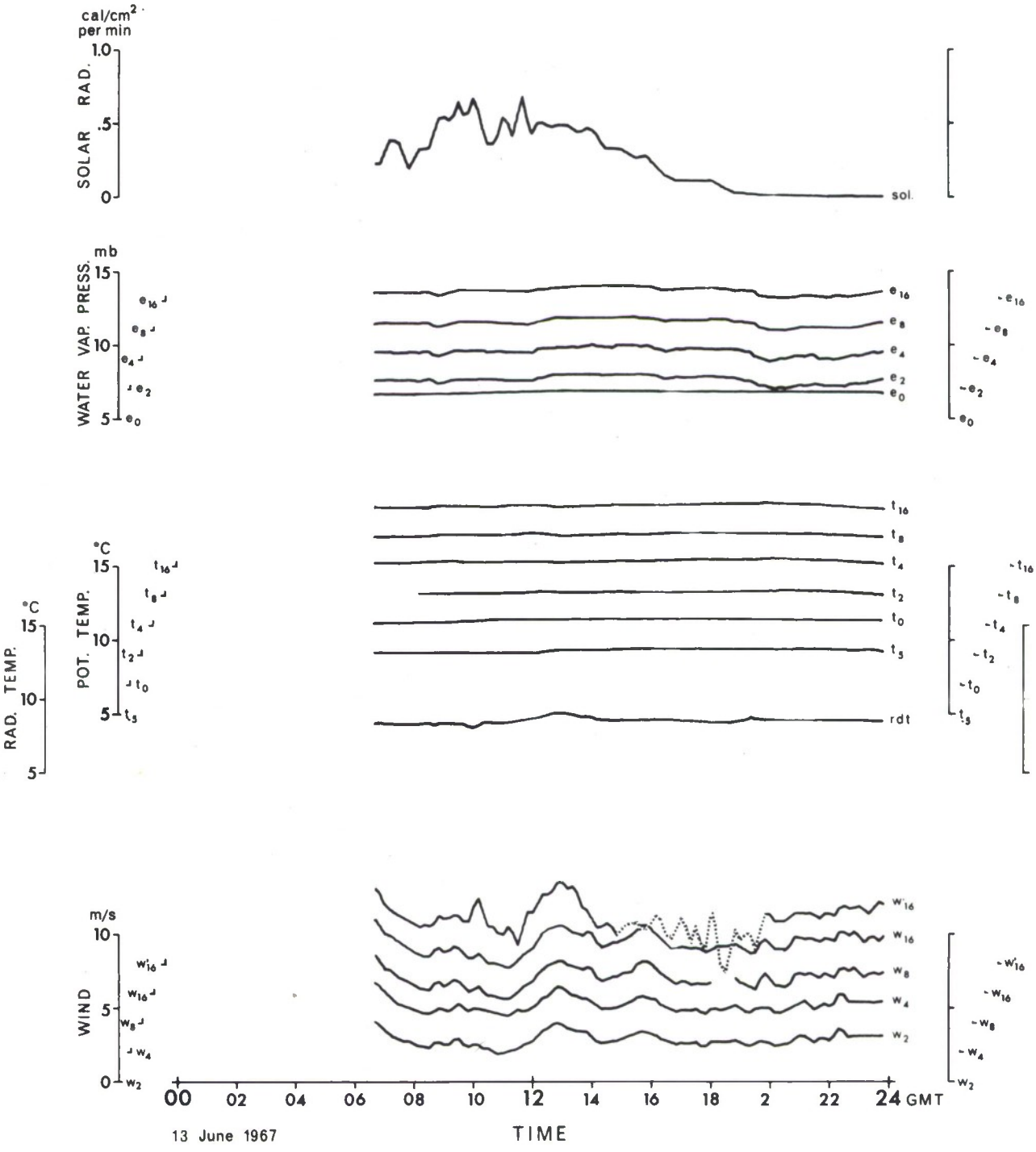
cal/cm² per min
SOLAR RAD.
1.0
.5
0
sol.
mb
WATER VAP. PRESS.
15
10
5
e16
e8
e4
e2
e0
°C
POT. TEMP.
15
10
5
t16
t8
t4
t2
t0
t5
rdt
°C
RAD. TEMP.
15
10
5
m/s
WIND
10
5
0
w'16
w16
w8
w4
w2
00 02 04 06 08 10 12 14 16 18 2 22 24 GMT
13 June 1967
TIME

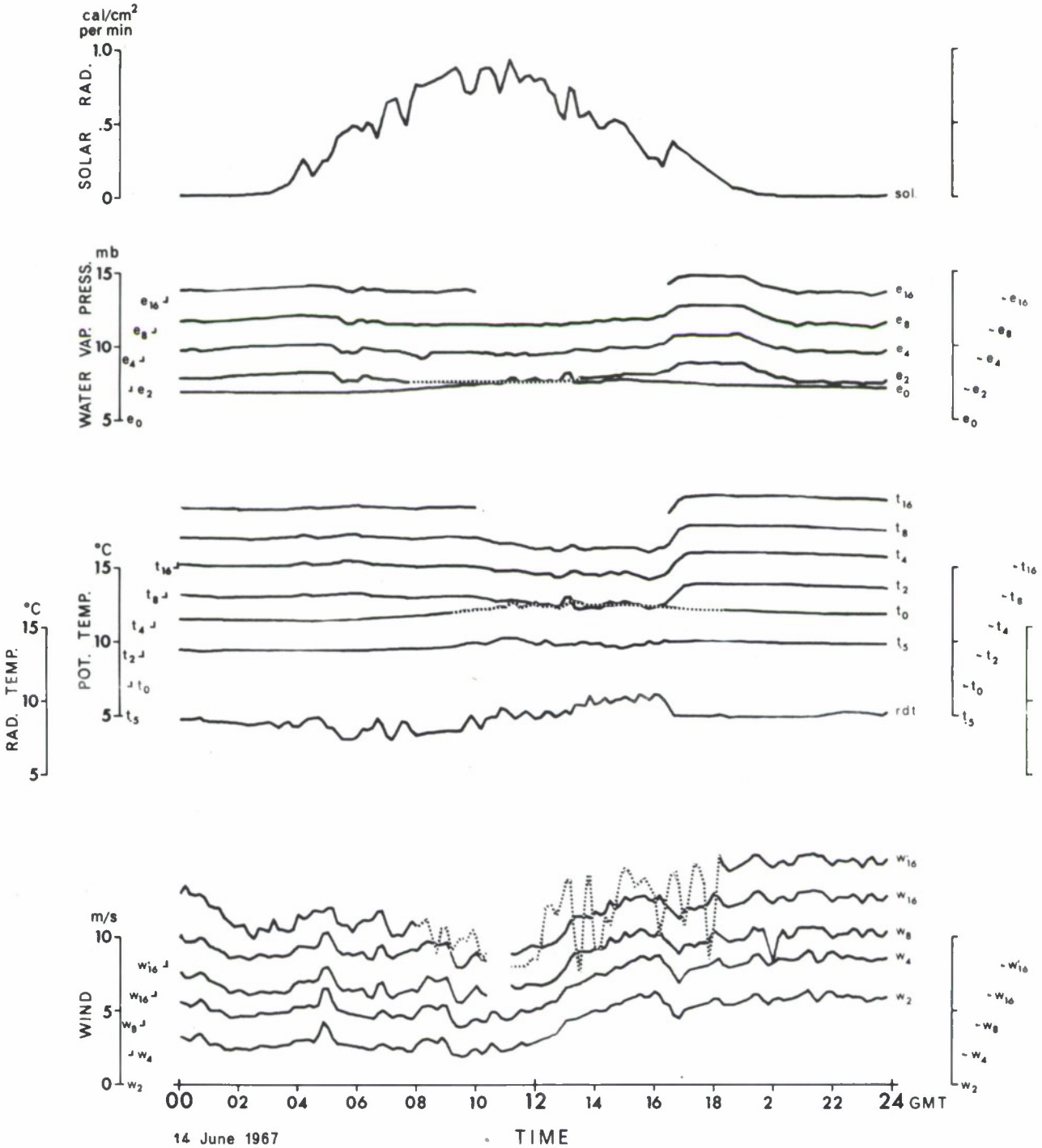
cal/cm² per min
SOLAR RAD.
1.0
.5
0
sol
mb
WATER VAP. PRESS.
15
10
5
e16
e8
e4
e2
e0
°C
POT. TEMP.
t16
t8
t4
t2
t0
t5
rdt
RAD. TEMP.
m/s
WIND
wi16
w16
w8
w4
w2
00 02 04 06 08 10 12 14 16 18 2 22 24 GMT
14 June 1967
TIME

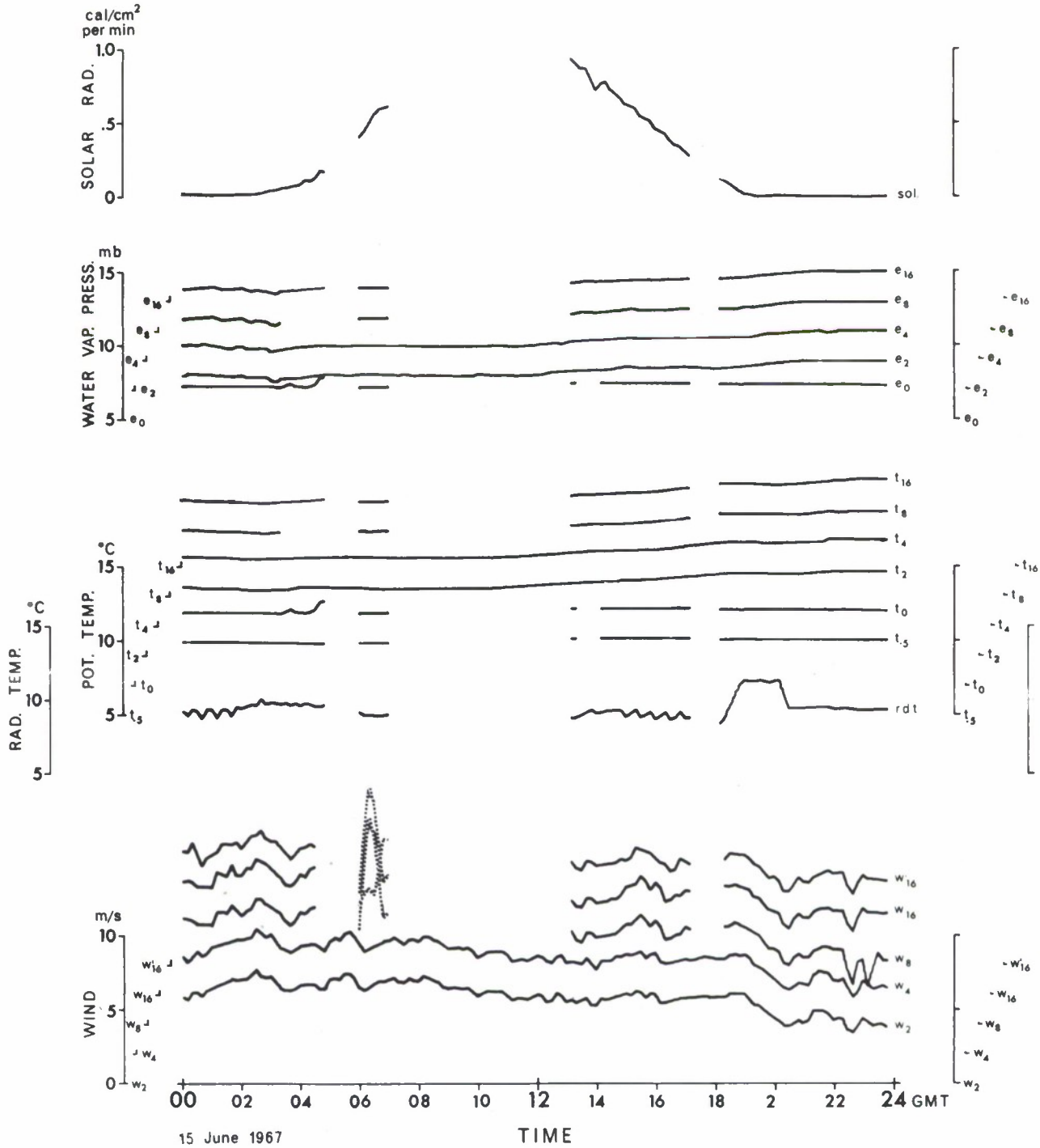
cal/cm² per min
SOLAR RAD.
1.0
.5
0
sol
mb
WATER VAP. PRESS.
15
10
5
e16
e8
e4
e2
e0
°C
POT. TEMP.
t16
t8
t4
t2
t0
t.5
rdt
°C
RAD. TEMP.
m/s
WIND
w16
w8
w4
w2
00 02 04 06 08 10 12 14 16 18 2 22 24 GMT
15 June 1967
TIME

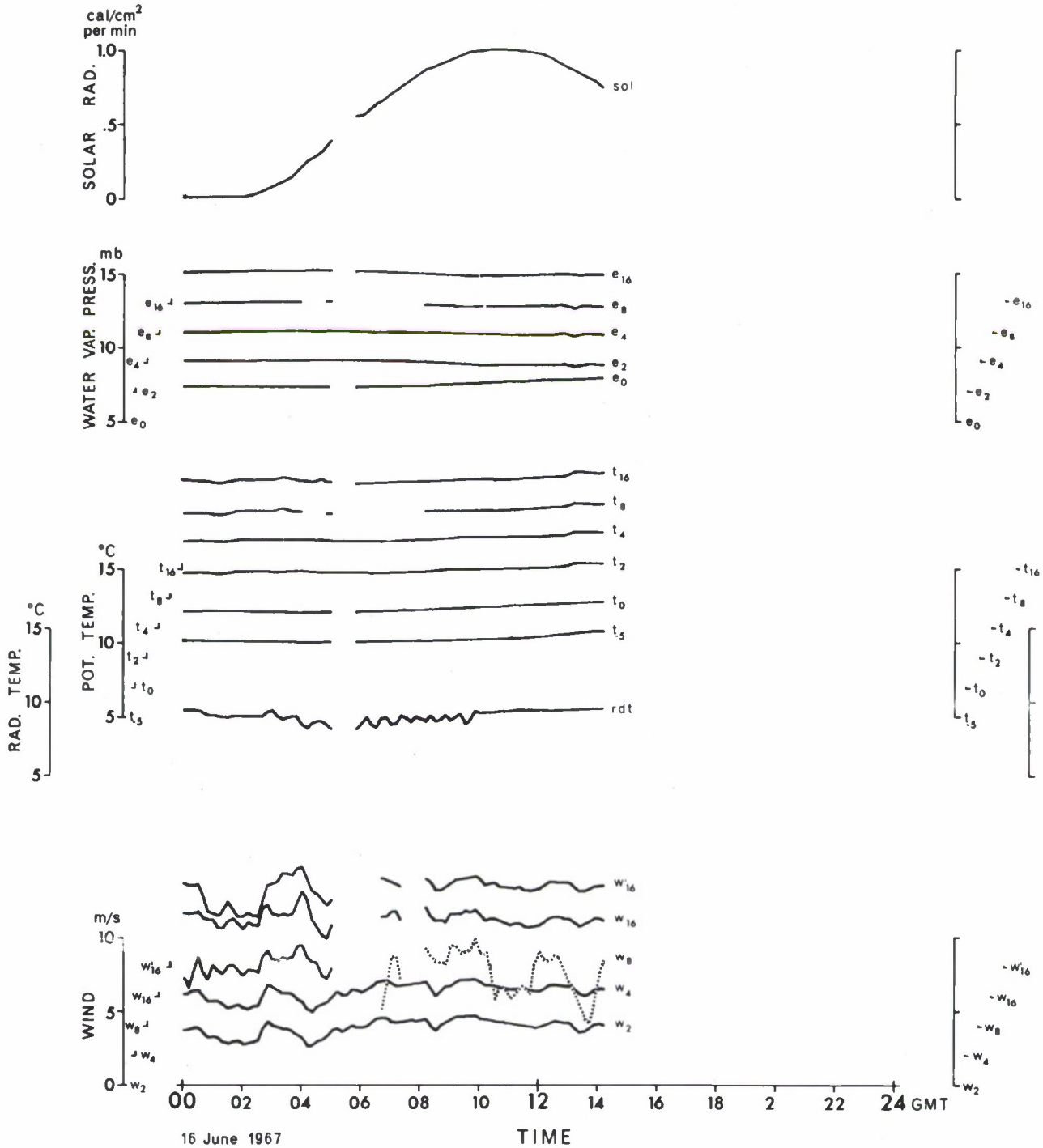
cal/cm² per min
SOLAR RAD.
1.0
.5
0
sol
mb
WATER VAP. PRESS.
15
10
5
e16
e8
e4
e2
e0
°C
POT. TEMP.
t16
t8
t4
t2
t0
t5
rdt
°C
RAD. TEMP.
m/s
WIND
w16
w8
w4
w2
00
02
04
06
08
10
12
14
16
18
2
22
24 GMT
16 June 1967
TIME

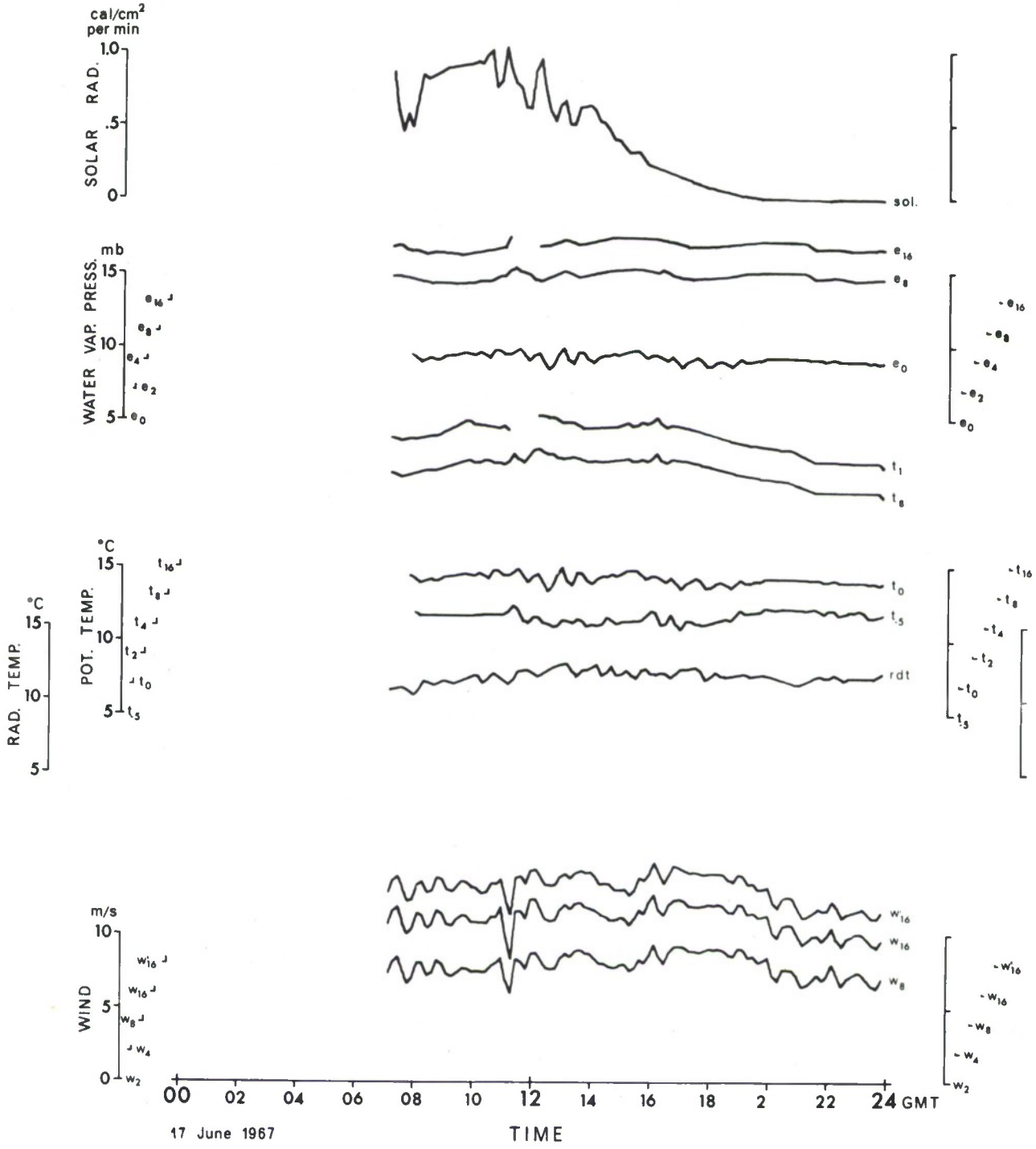
cal/cm² per min
SOLAR RAD.
1.0
.5
0
sol.
mb
WATER VAP. PRESS.
15
10
5
e16
e8
e4
e2
e0
°C
POT. TEMP.
t16
t8
t4
t2
t0
t5
t1
rdt
RAD. TEMP.
m/s
WIND
w16
w8
w4
w2
00
02
04
06
08
10
12
14
16
18
2
22
24 GMT
17 June 1967
TIME

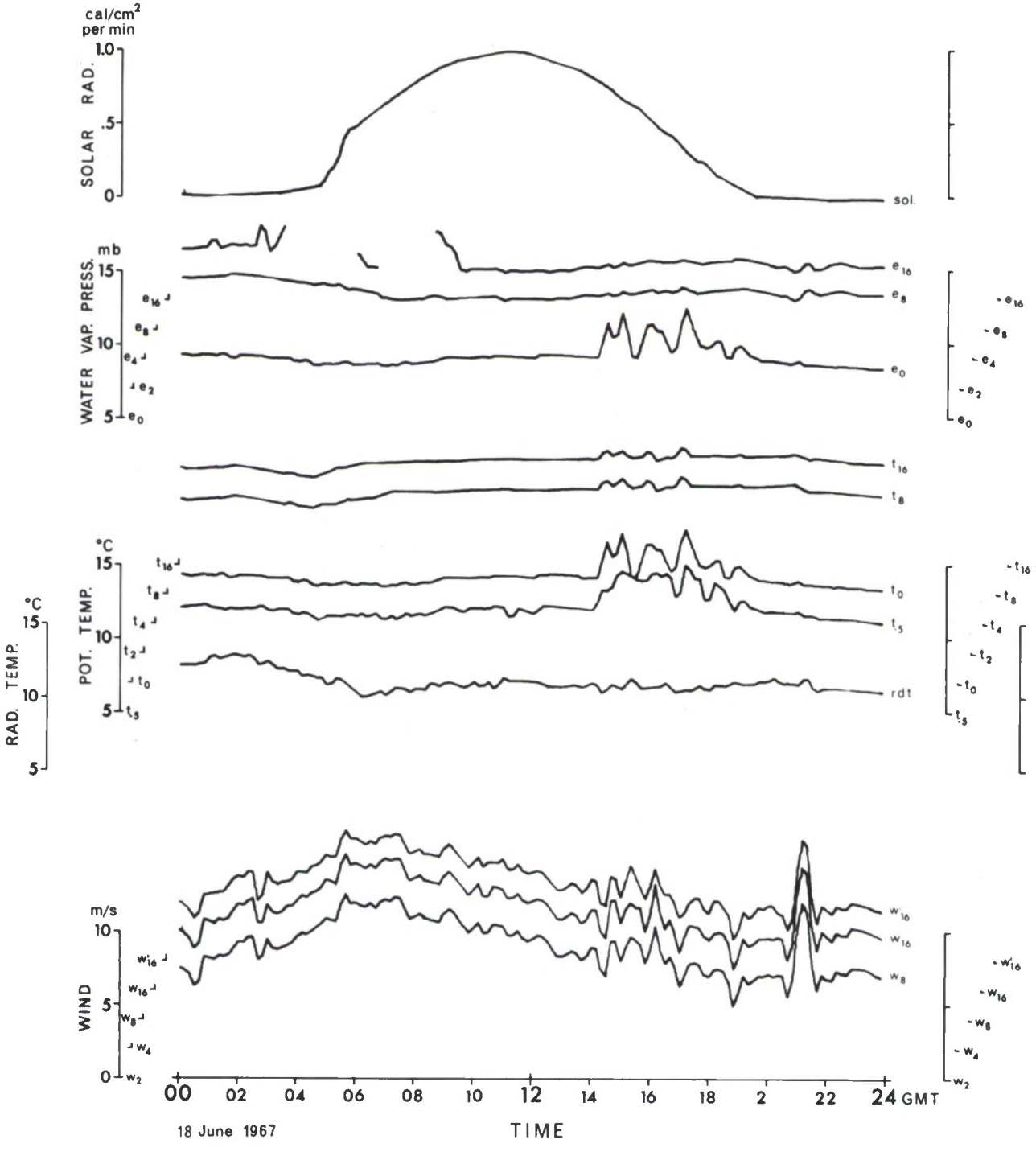
cal/cm² per min
SOLAR RAD.
1.0
.5
0
sol.
mb
WATER VAP. PRESS.
15
10
5
e16
e8
e4
e2
e0
°C
POT. TEMP.
t16
t8
t4
t2
t0
t5
rdt
RAD. TEMP.
m/s
WIND
w16
w8
w4
w2
00
02
04
06
08
10
12
14
16
18
2
22
24 GMT
18 June 1967
TIME

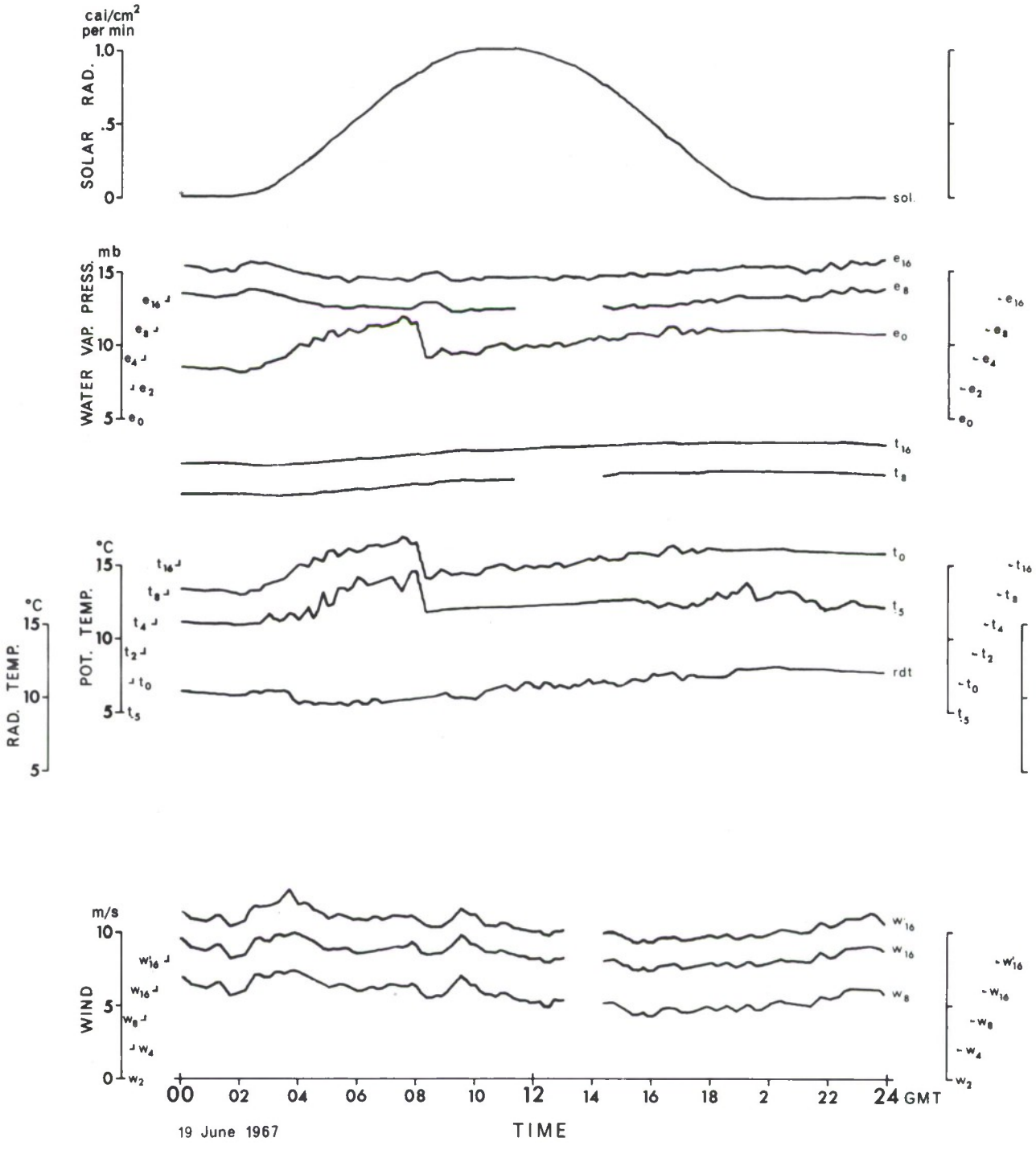
cal/cm² per min
SOLAR RAD.
1.0
.5
0
sol.
mb
WATER VAP. PRESS.
15
10
5
e16
e8
e4
e2
e0
°C
POT. TEMP.
t16
t8
t4
t2
t0
t5
rdt
RAD. TEMP.
m/s
WIND
w16
w8
w4
w2
00
02
04
06
08
10
12
14
16
18
2
22
24 GMT
19 June 1967
TIME

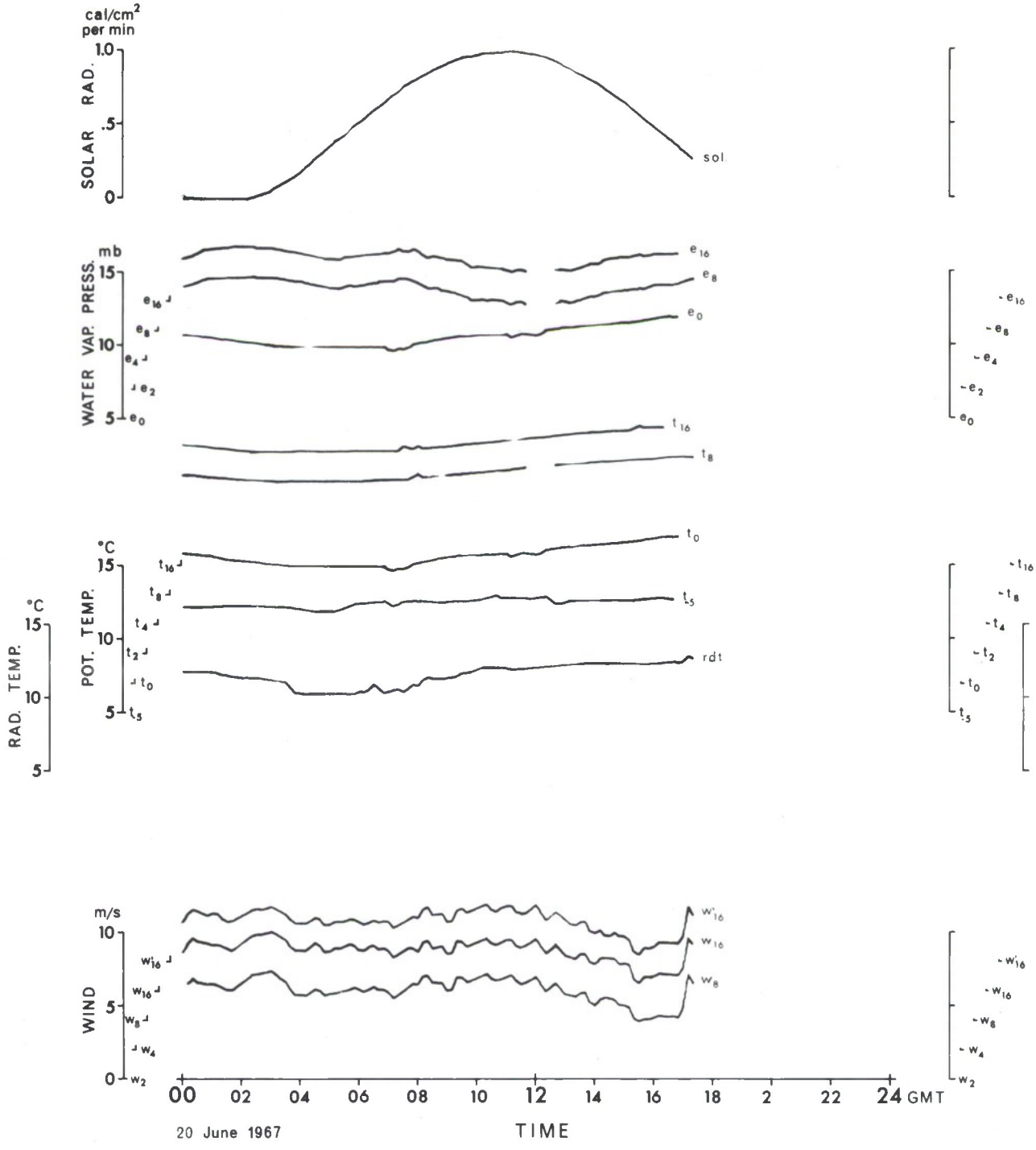
cal/cm² per min
SOLAR RAD.
1.0
.5
0
sol
mb
WATER VAP. PRESS.
15
10
5
e16
e8
e4
e2
e0
°C
POT. TEMP.
t16
t8
t4
t2
t0
t5
rdt
RAD. TEMP.
m/s
WIND
w16
w8
w4
w2
00
02
04
06
08
10
12
14
16
18
2
22
24 GMT
20 June 1967
TIME

EXAMPLE OF COMPUTER PRINTOUT OF PROCESSED DATA

FROM 0000 TO 0550 ON 8 JUNE 1967

Day	Hour	Minute	Pot. temp., °C, dry-bulb, at 16 m	Pot. temp., °C, wet-bulb, at 16 m	Pot. temp., °C, virtual, at 16 m	Vapour pressure, mb, at 16 m	Wind speed, m/s, at 16 m	Pot. temp., °C, dry-bulb, at 8 m	Pot. temp., °C, wet-bulb, at 8 m	Pot. temp., °C, virtual, at 8 m	Vapour pressure, mb, at 8 m	Wind speed, m/s, at 8 m	Temperature, °C, at sea surface	Virtual temperature, °C, at sea surface	Vapour pressure, mb, at sea surface
08	00	00	10.400	9.930	11.683	11.912	6.837	10.224	9.825	11.502	11.874	5.595	9.148	10.391	11.552
08	00	10	10.376	9.919	11.659	11.911	6.375	10.217	9.828	11.496	11.882	5.374	9.149	10.393	11.553
08	00	20	10.372	9.931	11.658	11.931	7.022	10.222	9.840	11.503	11.896	5.955	9.148	10.392	11.552
08	00	30	10.306	9.893	11.590	11.919	6.671	10.150	9.800	11.430	11.885	5.634	9.148	10.392	11.552
08	00	40	10.273	9.885	11.553	11.931	6.504	10.111	9.794	11.392	11.901	5.439	9.148	10.392	11.552
08	00	50	10.291	9.912	11.578	11.957	7.280	10.134	9.822	11.418	11.928	6.125	9.146	10.390	11.551
08	01	00	10.225	9.871	11.510	11.941	7.097	10.078	9.787	11.360	11.912	6.054	9.142	10.385	11.547
08	01	10	10.193	9.864	11.479	11.950	7.152	10.054	9.787	11.338	11.929	6.090	9.145	10.389	11.550
08	01	20	10.209	9.877	11.497	11.959	6.913	10.063	9.797	11.348	11.937	5.812	9.144	10.387	11.549
08	01	30	10.177	9.836	11.460	11.920	6.558	10.020	9.750	11.300	11.898	5.389	9.139	10.382	11.545
08	01	40	10.136	9.775	11.412	11.858	6.406	9.977	9.692	11.251	11.842	5.223	9.139	10.382	11.545
08	01	50	10.105	9.705	11.372	11.774	5.949	9.944	9.622	11.209	11.759	4.863	9.136	10.379	11.542
08	02	00	10.163	9.680	11.423	11.699	5.762	10.006	9.591	11.262	11.674	4.646	9.139	10.382	11.545
08	02	10	10.174	9.662	11.430	11.666	5.885	10.032	9.578	11.284	11.637	4.872	9.137	10.380	11.543
08	02	20	10.076	9.605	11.329	11.643	5.938	9.939	9.533	11.190	11.633	4.927	9.136	10.379	11.543
08	02	30	10.091	9.590	11.341	11.615	6.315	9.940	9.512	11.188	11.601	5.263	9.135	10.378	11.542
08	02	40	10.065	9.560	11.312	11.589	6.522	9.933	9.493	11.179	11.578	5.545	9.133	10.376	11.540
08	02	50	9.962	9.498	11.206	11.567	6.206	9.849	9.447	11.093	11.566	5.349	9.134	10.377	11.541
08	03	00	9,931	9.457	11.171	11.527	6.450	9.814	9.403	11.053	11.526	5.453	9.132	10.374	11.539
08	03	10	9.940	9.432	11.176	11.484	6.436	9.822	9.375	11.056	11.480	5.394	9.133	10.375	11.540
08	03	20	9.930	9.408	11.162	11.456	6.338	9.810	9.346	11.041	11.445	5.350	9.130	10.373	11.538
08	03	30	9.912	9.380	11.141	11.428	6.205	9.792	9.323	11.021	11.424	5.220	9.128	10.370	11.537
08	03	40	9.896	9.348	11.121	11.391	5.398	9.776	9.308	11.003	11.412	4.888	9.128	10.370	11.536
08	03	50	9.849	9.334	11.076	11.402	6.217	9.729	9.279	10.955	11.401	5.169	9.125	10.368	11.525
08	04	00	9.847	9.304	11.068	11.360	6.570	9.732	9.246	10.952	11.352	5.567	9.122	10.363	11.532
08	04	10	9.888	9.328	11.111	11.367	6.653	9.778	9.223	10.992	11.289	5.694	9.123	10.365	11.533
08	04	20	9.912	9.324	11.132	11.346	6.926	9.794	9.217	11.006	11.269	5.972	9.117	10.359	11.528
08	04	30	9.934	9.257	11.144	11.250	7.238	9.826	9.205	11.034	11.231	6.340	9.114	10.355	11.526
08	04	40	9.976	9.248	11.180	11.194	7.688	9.876	9.202	11.080	11.192	6.788	9.117	10.358	11.528
08	04	50	9.958	9.299	11.171	11.279	7.891	9.852	9.209	11.058	11.219	6.845	9.114	10.354	11.525
08	05	00	9.945	9.306	11.161	11.297	7.922	9.847	9.168	11.048	11.163	6.889	9.111	10.352	11.523
08	05	10	9.955	9.245	11.161	11.202	7.721	9.863	9.130	11.056	11.097	6.887	9.109	10.349	11.522
08	05	20	9.928	9.165	11.122	11.106	7.567	9.831	9.091	11.021	11.062	6.687	9.107	10.347	11.520
08	05	30	9.922	9.099	11.107	11.014	7.368	9.833	9.037	11.014	10.984	6.594	9.101	10.341	11.516
08	05	40	9.901	9.085	11.085	11.007	6.752	9.820	9.017	10.999	10.964	6.077	9.097	10.336	11.512
08	05	50	9.856	9.066	11.040	11.010	6.989	9.774	9.007	10.954	10.980	6.184	9.092	10.331	11.508

Day	Hour	Minute	Sea temperature 5 m below surface, °C	Sea surface radiation temp., °C	Wind speed at 16m, m/s (propeller-type anemometer)	Solarimeter output, cal/(cm^2.min)	Radiation balance probe output, cal/(cm^2.min)	Ship speed, m/s rel. to surface	Relative wind direction, degrees	Ship heading, degrees	Pot. temp., °C, dry-bulb, at 4 m	Pot. temp., °C, wet-bulb, at 4 m	Pot. temp., °C, virtual, at 4 m	Vapour pressure, mb, at 4 m	Wind speed, m/s, at 4 m	Pot. temp., °C, dry-bulb, at 2 m	Pot. temp., °C, wet-bulb, at 2 m	Pot. temp., °C, virtual, at 2 m	Vapour pressure, mb, at 2 m	Wind speed, m/s, at 2 m
08	00	00	9.150	10.070	7.554	-0.010	-0.013	-0.050	214	228	10.320	9.857	11.597	11.857	6.063	10.148	9.823	11.431	11.920	5.455
08	00	10	9.152	10.544	6.655	-0.011	-0.011	-0.050	179	270	10.296	9.846	11.573	11.856	5.023	10.120	9.820	11.405	11.934	5.171
08	00	20	9.150	10.155	6.847	-0.011	-0.015	-0.050	209	236	10.260	9.834	11.538	11.862	5.910	10.103	9.810	11.337	11.931	5.277
08	00	30	9.152	10.201	6.600	-0.013	-0.019	-0.050	193	252	10.200	9.814	11.479	11.872	5.777	10.039	9.771	11.321	11.915	5.215
08	00	40	9.151	10.196	6.531	-0.010	-0.023	-0.049	202	247	10.212	9.839	11.493	11.902	5.801	10.040	9.795	11.326	11.951	5.255
08	00	50	9.140	10.146	7.054	-0.010	-0.029	-0.052	206	245	10.210	9.852	11.494	11.922	6.315	10.053	9.812	11.340	11.966	5.689
08	01	00	9.145	10.346	7.032	-0.012	-0.026	-0.044	183	257	10.182	9.837	11.465	11.918	6.519	10.022	9.792	11.309	11.957	5.871
08	01	10	9.147	10.529	6.984	-0.012	-0.016	-0.040	206	246	10.128	9.800	11.409	11.899	6.155	9.970	9.759	11.255	11.943	5.579
08	01	20	9.148	10.608	6.999	-0.013	-0.021	-0.043	192	260	10.099	9.805	11.382	11.926	5.779	9.946	9.741	11.229	11.933	5.194
08	01	30	9.147	9.805	6.499	-0.012	-0.043	-0.036	204	248	10.120	9.801	11.402	11.905	5.647	9.948	9.736	11.231	11.924	5.063
08	01	40	9.146	9.875	6.505	-0.012	-0.062	-0.032	189	261	10.078	9.717	11.350	11.810	5.547	9.900	9.679	11.177	11.871	5.000
08	01	50	9.143	9.694	6.045	-0.012	-0.064	-0.036	200	251	10.036	9.646	11.299	11.733	5.062	9.870	9.622	11.140	11.809	4.569
08	02	00	9.146	9.684	5.739	-0.013	-0.064	-0.045	200	254	10.071	9.618	11.327	11.669	5.043	9.918	9.607	11.182	11.754	4.574
08	02	10	9.143	9.824	5.968	-0.010	-0.059	-0.038	191	263	10.069	9.595	11.322	11.636	5.227	9.926	9.578	11.186	11.707	4.725
08	02	20	9.142	9.525	5.850	-0.001	-0.067	-0.037	201	253	9.995	9.557	11.247	11.630	4.919	9.833	9.526	11.090	11.691	4.427
08	02	30	9.144	9.867	6.368	0.005	-0.066	-0.040	191	264	9.995	9.533	11.243	11.595	5.340	9.824	9.512	11.080	11.678	4.832
08	02	40	9.141	9.739	6.446	0.012	-0.032	-0.023	199	259	9.970	9.502	11.214	11.567	5.465	9.819	9.496	11.072	11.658	4.957
08	02	50	9.139	8.610	6.221	0.019	-0.010	-0.023	192	268	9.913	9.472	11.156	11.560	5.392	9.762	9.464	11.014	11.648	4.890
08	03	00	9.138	7.434	6.407	0.032	-0.005	-0.013	200	263	9.907	9.447	11.147	11.528	5.840	9.761	9.442	11.010	11.616	5.293
08	03	10	9.136	7.505	6.400	0.053	0.006	-0.012	197	270	9.913	9.423	11.149	11.489	5.809	9.772	9.416	11.016	11.572	5.277
08	03	20	9.125	7.654	6.300	0.051	0.006	-0.005	197	270	9.890	9.391	11.122	11.458	5.583	9.745	9.383	10.986	11.542	5.055
08	03	30	9.135	8.099	6.217	0.065	0.037	-0.004	192	273	9.884	9.368	11.113	11.428	5.436	9.730	9.371	10.969	11.534	4.916
08	03	40	9.129	8.143	5.921	0.106	0.085	0.006	192	271	9.889	9.353	11.116	11.403	5.111	9.727	9.367	10.966	11.530	4.640
08	03	50	9.127	7.732	6.173	0.085	0.056	0.003	194	267	9.843	9.338	11.071	11.412	5.348	9.694	9.336	10.931	11.508	4.834
08	04	00	9.126	7.519	6.580	0.123	0.080	0.017	194	271	9.821	9.307	11.044	11.381	5.741	9.681	9.312	10.915	11.480	5.226
08	04	10	9.125	7.559	6.603	0.154	0.109	0.041	195	273	9.856	9.274	11.072	11.311	5.857	9.716	9.303	10.946	11.444	5.369
08	04	20	9.122	7.678	6.878	0.135	0.077	0.024	191	276	9.908	9.277	11.121	11.281	6.097	9.760	9.298	10.987	11.408	5.587
08	04	30	9.121	7.653	7.235	0.261	0.183	0.028	193	274	9.930	9.261	11.139	11.243	6.498	9.776	9.299	11.003	11.399	5.959
08	04	40	9.117	8.211	7.711	0.340	0.267	0.018	189	277	9.955	9.257	11.162	11.220	6.921	9.805	9.294	11.028	11.373	6.326
08	04	50	9.110	8.529	7.794	0.253	0.221	0.016	190	275	9.958	9.269	11.166	11.236	7.006	9.818	9.306	11.042	11.383	6.354
08	05	00	9.109	8.015	7.828	0.266	0.213	0.052	190	278	9.962	9.235	11.165	11.185	7.316	9.819	9.288	11.040	11.355	6.641
08	05	10	9.107	7.577	7.766	0.369	0.295	0.047	187	281	9.944	9.192	11.141	11.134	7.067	9.805	9.238	11.019	11.292	6.437
08	05	20	9.104	7.527	7.597	0.400	0.364	0.029	189	278	9.902	9.151	11.096	11.102	6.648	9.762	9.204	10.974	11.270	6.041
08	05	30	9.096	7.562	7.497	0.419	0.384	0.032	185	282	9.917	9.108	11.104	11.030	6.680	9.777	9.172	10.983	11.215	6.067
08	05	40	9.090	7.696	6.983	0.441	0.423	-0.014	179	281	9.916	9.097	11.101	11.015	6.385	9.786	9.155	10.989	11.185	5.810
08	05	50	9.085	7.625	7.213	0.462	0.462	-0.030	178	276	9.876	9.082	11.061	11.021	6.651	9.751	9.140	10.954	11.185	6.058

APPENDIX B

CALCULATED FLUXES

Time GMT	Momentum Flux τ g/(cm·s)	Sensible Heat Flux H cal/cm²	Latent Heat Flux E cal/cm²	Solar Radiation Flux S cal/cm²
7/6/67				
13	5380	4.3	2.9	35.4
14	6620	4.8	3.3	30.9
15	2630	2.0	1.3	25.2
16	1150	1.2	0.7	21.7
17	1460	1.2	0.6	12.0
18	1190	0.9	0.5	6.2
19	1350	0.8	0.6	1.2
20	2150	1.1	0.6	0.0
21	2980	1.4	0.5	0.0
22	4040	1.5	0.6	0.0
23	3420	1.4	0.5	0.0
8/6/67				
00	3000	1.1	0.6	0.0
01	2970	1.0	0.5	0.0
02	2450	0.8	0.1	0.8
03	2660	0.7	-0.1	4.6
04	3580	0.8	-0.4	13.4
05	3820	0.9	-0.7	24.3
06	4330	0.8	-1.3	32.7
07	3950	0.8	-1.0	38.7
08	3770	1.0	-0.7	45.4
09	3940	1.1	-0.7	48.9

Time GMT	Momentum Flux τ g/(cm.s)	Sensible Heat Flux H cal/cm²	Latent Heat Flux E cal/cm²	Solar Radiation Flux S cal/cm²
8/6/67				
10	5480	1.5	-0.9	47.6
11	6220	1.7	-1.1	49.9
12	6660	1.9	-1.3	48.1
13	7330	2.3	-1.6	43.4
14	8350	2.6	-1.9	37.4
15	7300	2.4	-1.8	27.2
16	6550	2.2	-1.5	19.9
17	6390	2.5	-1.2	14.6
18	5730	2.3	-0.7	6.2
19	5710	2.2	-0.6	1.1
20	4270	1.8	-0.4	0.0
21	4040	2.0	-0.7	0.0
22	3780	1.7	-0.5	0.0
23	3750	1.5	-0.6	0.0
9/6/67				
00	3890	1.4	-0.7	0.0
01	4940	1.5	-0.6	0.0
02	5220	1.2	-0.9	1.8
03	4610	1.0	-0.8	7.1
04	4760	0.8	-0.9	16.3
05	4730	0.7	-0.9	24.8
06	3630	0.6	-0.8	32.5
07	3260	0.4	-1.2	39.6
08	3300	0.3	-1.6	42.0
09	3660	0.3	-1.9	46.6
10	4430	0.4	-2.5	50.9
11	3900	0.3	-3.0	50.7
12	4040	0.3	-2.6	48.2
13	4660	0.6	-2.3	43.3
14	5470	0.9	-2.6	37.7
15	7010	1.4	-3.0	32.3

Time GMT	Momentum Flux τ g/(cm·s)	Sensible Heat Flux H cal/cm²	Latent Heat Flux E cal/cm²	Solar Radiation Flux S cal/cm²
13/6/67				
06	1750	-0.2	-1.5	12.2
07	990	-0.1	-1.2	17.8
08	610	-0.1	-1.0	21.0
09	650	-0.1	-1.0	32.7
10	450	-0.2	-0.8	27.4
11	430	-0.1	-0.9	31.1
12	1340	-0.3	-1.2	27.9
13	1410	-0.4	-1.2	27.1
14	980	-0.2	-0.9	21.4
15	1410	-0.3	-1.1	16.3
16	1060	-0.2	-1.1	9.1
17	750	-0.1	-0.9	5.9
18	860	-0.1	-1.0	3.6
19	810	-0.1	-1.3	0.4
20	880	-0.1	-1.6	0.2
21	1130	-0.2	-1.7	0.0
22	1290	-0.3	-1.8	0.0
23	1190	-0.3	-1.4	0.0
14/6/67				
00	1120	-0.4	-1.3	0.0
01	710	-0.4	-1.0	0.0
02	580	-0.3	-0.8	0.6
03	630	-0.3	-0.7	3.7
04	970	-0.3	-0.8	11.7
05	870	-0.2	-1.0	22.6
06	730	-0.3	-1.0	27.4
07	710	-0.5	-1.3	35.7
08	1010	-0.6	-1.7	45.7
09	600	-0.6	-1.4	47.0
10	790	-0.8	-1.9	43.1

Time GMT	Momentum Flux τ g/(cm·s)	Sensible Heat Flux H cal/cm²	Latent Heat Flux E cal/cm²	Solar Radiation Flux S cal/cm²
14/6/67				
11				
12				
13				
14				
15				
16	2470	-1.3	-1.8	19.7
17	2780	-0.4	-1.3	14.2
18	3080	-0.3	-1.3	5.7
19	3450	-0.3	-2.0	0.0
20	3320	-0.2	-2.8	0.0
21	3720	-0.3	-3.1	0.0
22	3400	-0.4	-3.0	0.0
23	3380	-0.4	-3.1	0.0
15/6/67				
00	4200	-0.8	-2.8	0.0
01	4960	-0.9	-3.2	0.0
02	5740	-1.1	-3.6	0.9
03	4700	-0.9	-3.6	2.9
04	5260	-0.8	-3.3	6.0
05				
06	(8980)	(-1.1)	(-3.9)	(30.5)*
07	(5030)	(-0.8)	(-2.9)	(36.3)*
08				
09				
10				
11				
12				

* Doubtful values

Time GMT	Momentum Flux τ g/(cm·s)	Sensible Heat Flux H cal/cm²	Latent Heat Flux E cal/cm²	Solar Radiation Flux S cal/cm²
15/6/67				
13	2930	-0.5	-2.1	54.5
14	3200	-0.4	-2.0	43.2
15	4310	-0.5	-2.2	33.7
16	3560	-0.2	-1.9	23.5
17	3760	0.1	-1.8	16.8
18	4000	0.5	-1.7	4.2
19	3140	0.4	-1.2	0.3
20	1920	0.3	-0.6	0.2
21	2190	0.5	-0.5	0.0
22	1830	0.6	-0.4	0.0
23	2090	0.6	-0.4	0.0
16/6/67				
00	2000	0.6	-0.4	0.0
01	1580	0.5	-0.3	0.1
02	1750	0.6	-0.2	1.8
03	2050	0.8	-0.1	7.6
04	1870	0.6	-0.2	16.9
05	1710	0.5	-0.2	28.2
06	1990	0.5	-0.4	40.2
07	2140	0.5	-0.5	44.0
08	1920	0.6	-0.8	53.7
09	2260	0.6	-1.1	58.2
10	1890	0.4	-1.1	60.1
11	1610	0.3	-1.1	59.2
12	1920	0.4	-1.2	56.2
13	1760	0.5	-1.3	50.5
14	1900	0.5	-1.4	45.2

Time GMT	Momentum Flux τ g/(cm.s)	Sensible Heat Flux H cal/cm²	Latent Heat Flux E cal/cm²	Solar Radiation Flux S cal/cm²
17/6/67				
07	820	0.5	-0.7	28.7
08	1280	0.9	-0.6	48.2
09	1220	1.0	-0.9	53.7
10	1140	0.9	-0.7	53.5
11	1180	0.9	-0.4	56.3
12	1210	1.3	-0.2	40.8
13	1890	1.4	-0.4	35.5
14	1400	1.1	-0.1	28.9
15	1330	1.1	-0.2	18.1
16	1930	1.6	-0.1	11.1
17	1960	1.6	-0.2	6.6
18	1920	1.3	0.0	3.0
19	1930	0.8	0.0	0.7
20	1340	0.4	-0.2	0.1
21	1040	0.1	-0.4	0.0
22	1160	0.0	-0.6	0.0
23	1030	0.0	-0.5	0.0
18/6/67				
00	930	-0.4	-0.8	0.0
01	1740	-0.6	-0.6	0.0
02	2300	-0.8	-0.3	0.4
03	2180	-0.9	0.2	1.4
04				
05				
06	(5200)	(0.3)	(-2.7)	(33.1)*

* Doubtful values

Time GMT	Momentum Flux τ g/(cm·s)	Sensible Heat Flux H cal/cm²	Latent Heat Flux E cal/cm²	Solar Radiation Flux S cal/cm²
18/6/67				
07				
08	3780	-0.1	1.0	53.1
09	4060	-0.1	-2.6	56.0
10	3460	-0.1	-3.9	59.0
11	2980	-0.1	-3.9	59.1
12	2470	-0.3	-3.7	56.4
13	1830	-0.1	-2.8	51.9
14	2130	-0.9	-4.5	44.9
15	2190	-1.1	-4.5	36.4
16	2180	-1.4	-4.6	26.7
17	1280	-1.3	-4.3	16.6
18	920	-0.4	-2.1	8.0
19	760	0.0	-1.4	1.6
20	660	0.3	-1.0	0.2
21	2600	0.5	-1.9	0.0
22	970	0.3	-0.9	0.0
23	1040	0.3	-1.0	0.0
19/6/67				
00	420	0.2	-0.6	0.0
01	360	0.2	-0.5	0.0
02	580	0.1	-0.5	1.2
03	1110	-0.3	-2.2	7.0
04	1000	-1.0	-3.9	16.2
05	750	-1.3	-4.7	26.4
06	720	-1.4	-4.8	36.4
07	920	-1.7	-6.0	45.5
08	560	-0.3	-2.6	52.9
09	840	0.2	-2.8	58.4

Time GMT	Momentum Flux τ g/(cm.s)	Sensible Heat Flux H cal/cm²	Latent Heat Flux E cal/cm²	Solar Radiation Flux S cal/cm²
19/6/67				
10	630	0.0	-2.7	60.5
11	490	0.0	-2.5	60.1
12	390	0.0	-2.4	57.1
13	430	0.0	-2.2	54.1
14	400	-0.2	-2.7	43.4
15	230	-0.2	-2.3	35.6
16	290	-0.4	-2.7	25.6
17	300	-0.4	-2.6	15.5
18	330	-0.4	-2.7	6.5
19	360	-0.4	-2.7	0.5
20	450	-0.4	-3.1	0.0
21	490	-0.3	-3.1	0.0
22	680	-0.4	-3.1	0.0
23	790	-0.4	-3.1	0.0
20/6/67				
00	850	-0.5	-2.4	0.0
01	720	-0.4	-1.6	0.0
02	1080	-0.4	-1.6	0.2
03	930	-0.2	-1.4	6.5
04	680	-0.1	-1.6	15.6
05	720	-0.2	-1.7	25.7
06	670	-0.1	-1.4	35.6
07	550	0.0	-1.0	44.6
08	780	-0.3	-2.1	52.0
09	790	-0.4	-3.0	57.2
10	960	-0.4	-3.7	59.6
11	880	-0.2	-3.6	59.8
12	770	-0.3	-3.9	55.3
13	500	-0.2	-3.3	51.5
14	420	-0.2	-2.8	44.2
15	160	-0.1	-1.4	35.1
16	110	-0.1	-1.2	25.7

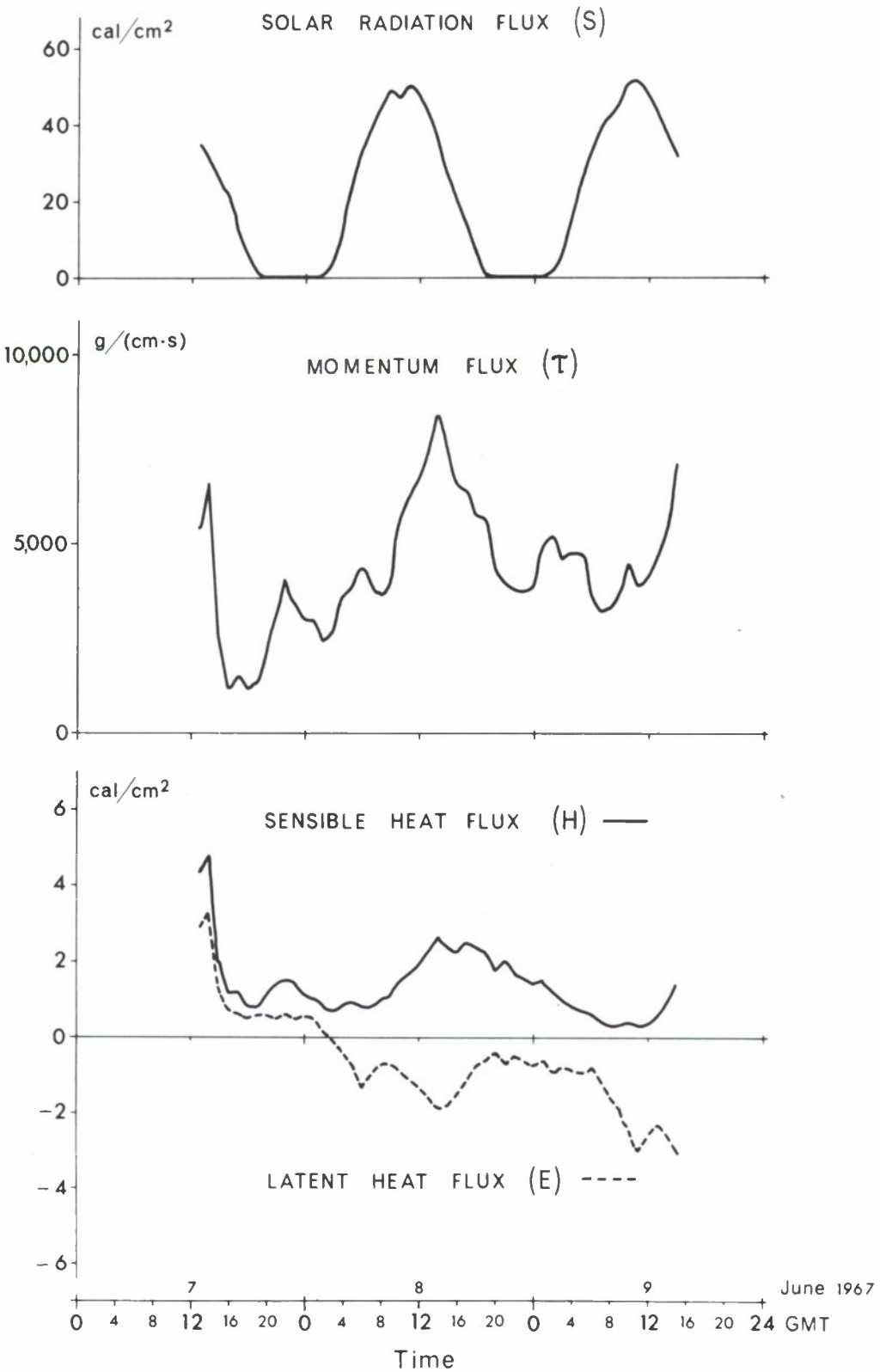
cal/cm²
SOLAR RADIATION FLUX (S)
60
40
20
0
g/(cm·s)
10,000
MOMENTUM FLUX (τ)
5,000
0
cal/cm²
6
SENSIBLE HEAT FLUX (H)
4
2
0
−2
−4
LATENT HEAT FLUX (E)
−6
7
8
9
June 1967
0 4 8 12 16 20 0 4 8 12 16 20 0 4 8 12 16 20 24 GMT
Time

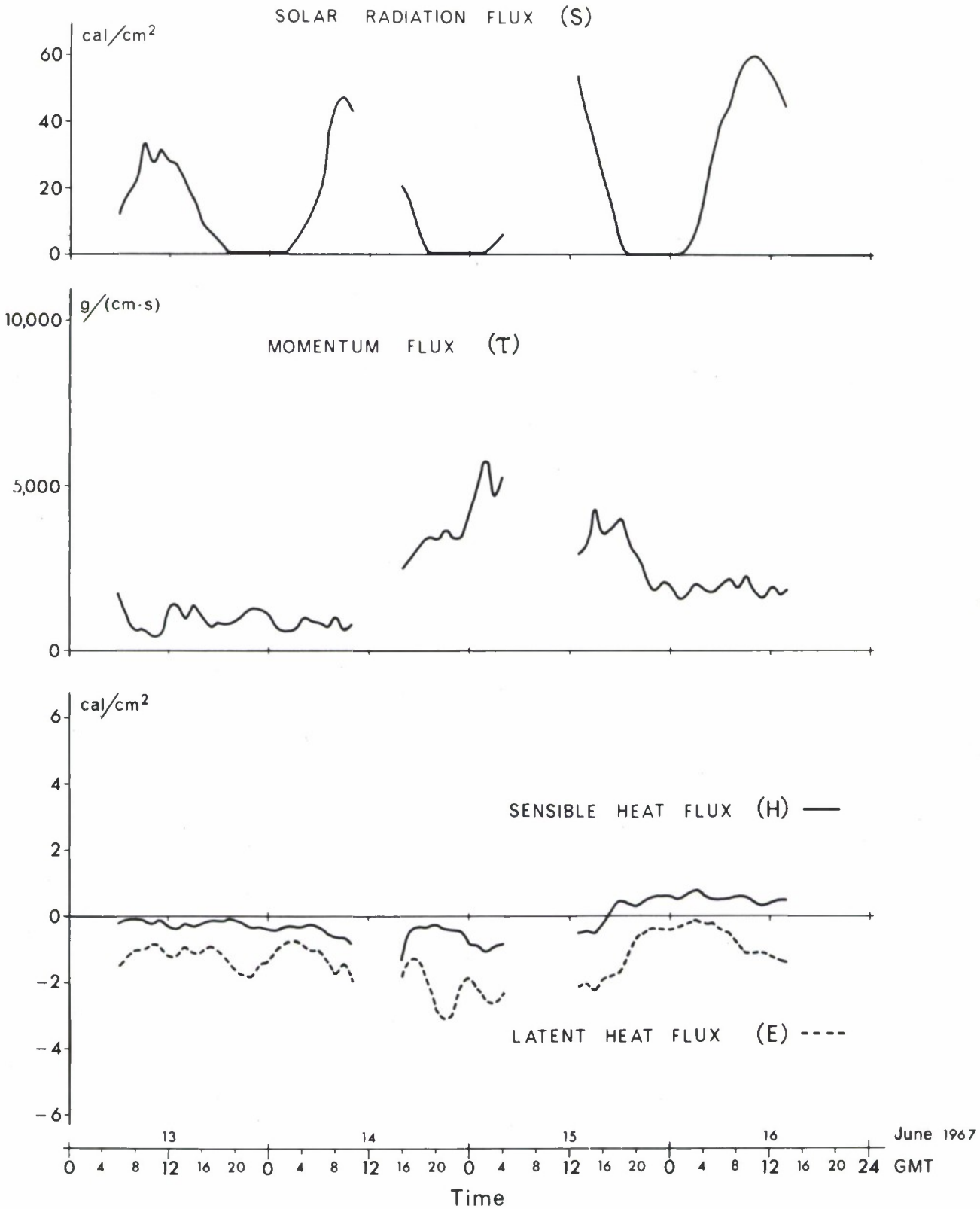
SOLAR RADIATION FLUX (S)
cal/cm²
60
40
20
0
g/(cm·s)
10,000
MOMENTUM FLUX (τ)
5,000
0
cal/cm²
6
4
2
0
-2
-4
-6
SENSIBLE HEAT FLUX (H)
LATENT HEAT FLUX (E)
13
14
15
16
June 1967
0 4 8 12 16 20 0 4 8 12 16 20 0 4 8 12 16 20 0 4 8 12 16 20 24
GMT
Time

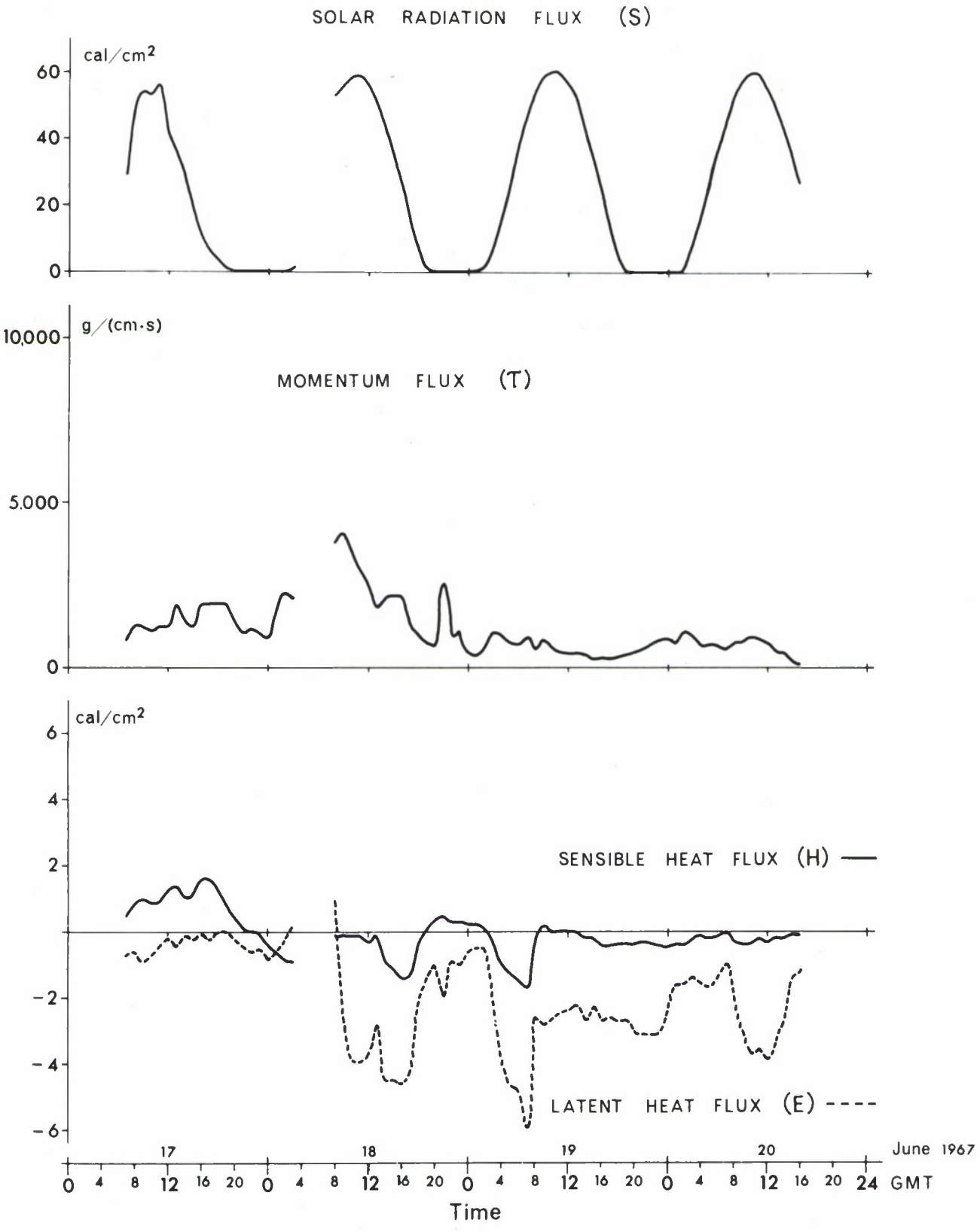
SOLAR RADIATION FLUX (S)
cal/cm²
60
40
20
0
g/(cm·s)
10,000
5,000
0
MOMENTUM FLUX (T)
cal/cm²
6
4
2
-2
-4
-6
SENSIBLE HEAT FLUX (H)
LATENT HEAT FLUX (E)
17
18
19
20
June 1967
0 4 8 12 16 20 0 4 8 12 16 20 0 4 8 12 16 20 0 4 8 12 16 20 24 GMT
Time

DISTRIBUTION

MINISTRIES OF DEFENCE	Copies
MOD Belgium	5
MOD Canada	10
MOD Denmark	10
MOD France	8
MOD Germany	13
MOD Greece	11
MOD Italy	10
MOD Netherlands	10
MOD Norway	10
MOD Portugal	5
MOD Turkey	3
MOD U.K.	20
SECDEF U.S.	71

NATO AUTHORITIES	
SECGEN NATO	3
NATO Military Committee	2
SACLANT	3
SACEUR	3
CINCHAN	1
SACLANTREPEUR	1
COMNAVSOUTH	1
CINCWESTLANT	1
COMSUBEASTLANT	1
COMCANLANT	1
COMOCEANLANT	1
COMEDCENT	1
COMSUBACLANT	1
COMSUBMED	1
CDR Task Force 442 (via COMSTRIKFORSOUTH)	1
COMMARAIRMED	1

SCNR for SACLANTCEN	Copies
SCNR Belgium	1
SCNR Canada	1
SCNR Denmark	1
SCNR Germany	1
SCNR Greece	1
SCNR Italy	1
SCNR Netherlands	1
SCNR Norway	1
SCNR Turkey	1
SCNR U.K.	1
SCNR U.S.	1

NATIONAL LIAISON OFFICERS	
NLO Italy	1
NLO Portugal	1
NLO U.K.	1
NLO U.S.	1

NLR to SACLANT	
NLR Belgium	1
NLR Canada	1
NLR Denmark	1
NLR Germany	1
NLR Greece	1
NLR Italy	1
NLR Norway	1
NLR Portugal	1
NLR Turkey	1
NLR U.K.	1